NASA
Technical Memorandum 78591

AVRADCOM
Technical Report 79-23

V/STOLAND Avionics System Flight-Test Data on a UH-1H Helicopter

Fredric A. Baker, Dean N. Jaynes, Lloyd D. Corliss,
Sam Liden, Robert B. Merrick, and Daniel C. Dugan

FEBRUARY 1980

NASA

U.S. ARMY AVRADCOM

NASA
Technical Memorandum 78591

AVRADCOM
Technical Report 79-23

V/STOLAND Avionics System Flight-Test Data on a UH-1H Helicopter

Fredric A. Baker and Dean N. Jaynes
Ames Research Center
Moffett Field, California

Lloyd D. Corliss
Aeromechanics Laboratory
AVRADCOM Research and Technology Laboratories
Ames Research Center, Moffett Field, California

Sam Liden
Sperry Rand Corporation
Phoenix, Arizona

Robert B. Merrick and Daniel C. Dugan
Ames Research Center
Moffett Field, California

National Aeronautics
and Space Administration

**Scientific and Technical
Information Office**

1980

NOTATION

A_{SS}	roll series servo command, deg
A_{IS}	lateral cyclic control input, deg
$\dot{A}_{PS}$	roll parallel servo command, deg/sec
a_y	lateral body acceleration, m/sec^2 (ft/sec^2)
B_{SS}	pitch series servo command, deg
B_{IS}	longitudinal cyclic control input, deg
$\dot{B}_{PS}$	pitch parallel servo command, deg/sec
C_{SS}	collective series servo command, deg
$\dot{C}_{PS}$	collective parallel servo command, deg/sec
D_{SS}	directional series servo command, deg
D_Y	cross-track displacement from reference flight path, ft
$\dot{D}_{PS}$	directional parallel servo command, deg/sec
$\dot{D}_Y$	cross-track rate, m/sec (ft/sec)
F_{FP}	pedal force, kg (lb)
F_{FPO}	pedal force threshold, kg (lb)
h	altitude (above ground), m (ft)
$\dot{h}$	altitude rate, m/sec (ft/sec)
$\ddot{h}$	altitude acceleration, m/sec^2 (ft/sec^2)
h_{FIN}	final hover altitude, m (ft)
$\dot{h}_{CF}$	filtered altitude rate command, m/sec (ft/sec)
$\dot{h}_c$	altitude rate command, m/sec (ft/sec)
$\dot{h}'_c$	raw altitude rate command, m/sec (ft/sec)
K_{AFF}	roll-rate feed-forward gain, deg/deg/sec

K_{APS} roll parallel servo gain, deg/sec/deg

K_{BFF} pitch rate feed-forward gain, deg/deg/sec

K_{BPS} pitch parallel servo gain, deg/sec/deg

K_{COL} collective sensitivity, m/sec/cm (ft/sec/in.)

K_{CPS} collective parallel servo gain, deg/sec/deg

K_{DFC} yaw/collective coupling gain, deg/deg

K_{DPS} directional parallel servo gain, deg/sec/deg

K_{Dp} yaw/roll coupling gain, deg/deg/sec

K_{FPH} pedal sensitivity, deg/sec/kg (deg/sec/lb)

K_{ay} Y body acceleration gain, deg/m/sec^2 (deg/ft/sec^2)

$K_{\dot{h}}$ altitude rate gain, deg/m/sec (deg/ft/sec)

$K_{\ddot{h}}$ altitude acceleration gain, deg/m/sec^2 (deg/ft/sec^2)

K_p roll rate gain, deg/deg/sec

K_q pitch rate gain, deg/deg/sec

K_r yaw rate gain, deg/deg/sec

K_{δ_θ} pitch sensitivity, deg/cm (deg/in.)

$K_{\delta_{\theta FF}}$ pitch stick feed-forward gain, deg/cm (deg/in.)

K_{δ_ϕ} roll sensitivity, deg/cm (deg/in.)

$K_{\delta_{\phi FF}}$ roll stick feed-forward gain, deg/cm (deg/in.)

K_θ pitch attitude gain, deg/deg

K_ϕ roll attitude gain, deg/deg

K_ψ heading gain, deg/deg

p roll rate, deg/sec

q pitch rate, deg/sec

r	yaw rate, deg/sec
r_c	yaw rate command, deg/sec
r'_{wo}	turn coordination, deg/sec
S	Laplace operator, 1/sec
V_{CF}	filtered airspeed command, m/sec (ft/sec)
V_G	ground speed, m/sec (ft/sec)
V_T	true airspeed, m/sec (ft/sec)
x	aircraft position (x-axis aligned with runway), m (ft)
y	aircraft position (y-axis), m (ft)
γ	aircraft computed flightpath angle, deg
γ_{CF}	filtered aircraft computed flightpath angle, deg
δ_{COL}	collective stick, cm (in.)
δ_θ	pitch cyclic stick position, cm (in.)
δ_ϕ	roll cyclic stick position, cm (in.)
θ	pitch attitude, deg
θ_{COL}	collective pitch, deg
θ_c	pitch attitude command, deg
θ'_c	raw pitch attitude command, deg
θ_{TR}	tilt rotor collective pitch, deg
ϕ	roll attitude, deg
ϕ_c	roll attitude command, deg
ϕ'_c	raw roll attitude command, deg
ψ	heading, deg
ψ_c	heading command, deg

ω	natural frequency, rad/sec
ζ	damping ratio, dimensionless
τ	time constant, sec
MLS	microwave landing system: provides angle and range information for landing
TACAN	tactical area navigation: a navigation aid that provides bearing and range information

V/STOLAND AVIONICS SYSTEM FLIGHT-TEST DATA ON A UH-1H HELICOPTER

Fredric A. Baker,* Dean N. Jaynes,* Lloyd D. Corliss,† Sam Liden,‡
Robert B. Merrick,* and Daniel C. Dugan*

Ames Research Center

SUMMARY

This report documents the flight-acceptance test results obtained during the acceptance tests of the V/STOLAND digital avionics system on a Bell UH-1H helicopter in 1977 at Ames Research Center. V/STOLAND is the acronym used for a versatile simplex digital avionics system developed and manufactured by Sperry Flight Systems Division of Sperry Rand Corporation. The system provides navigation, guidance, control, and display functions for NASA terminal area VTOL research programs and for the Army handling qualities research programs at Ames Research Center. The acceptance test verified system performance and contractual acceptability. The V/STOLAND hardware navigation, guidance, and control laws resident in the digital computers are described. Typical flight-test data are shown and discussed as documentation of the system performance at acceptance from the contractor.

INTRODUCTION

This report documents the results of the flight-acceptance tests of the V/STOLAND digital avionics system developed and manufactured by Sperry Flight Systems, Sperry Rand Corporation, and installed in a Bell UH-1H helicopter. The acceptance tests verified the system performance and its contractual acceptability. V/STOLAND is an experimental avionics system developed to provide sophisticated navigation, guidance, control, and display functions. Ames Research Center will use the system capability to vary terminal area navigation, guidance, and control functions; the Army will use it for handling qualities research.

The V/STOLAND system is similar to the STOLAND digital system previously developed by Sperry Flight Systems for installation on STOL aircraft at Ames Research Center. Many of the electronic units are interchangeable. The control augmentation system installation of parallel and series actuators is similar to several previous experimental systems on helicopters (e.g., HOVVAC, ALARMS, and HENILAS). V/STOLAND is a "single channel" system with no redundancy. Additional information on the system may be found in reference 1.

---

*Ames Research Center, Moffett Field, California 94035.

†Aeromechanics Laboratory, AVRADCOM Research and Technology Laboratories, Moffett Field, California 94035.

‡Sperry Flight Systems Division, Sperry Rand Corporation, Phoenix, Arizona 85002.

The acceptance tests consisted of tests both in a NASA simulator and in flight. The system performance was verified in the simulator by exercising all of the operating modes under a variety of controlled flight conditions. The system's failure monitors were also tested by injecting critical failures, such as servo hardovers and sensor failures, into the system. A failure is detected by a V/STOLAND failure monitor and, depending on its predetermined criticality, the monitor either automatically warns the pilot and disengages the servos or just warns the pilot with an alert light and message.

This report gives a brief description of the hardware and the guidance, navigation, and control laws that are resident software programs in the digital computer. Typical flight-test data are also shown and discussed with concluding remarks summarizing the results of the tests.

SYSTEM DESCRIPTION

The V/STOLAND system is a versatile integrated digital avionics system that provides navigation, guidance, control, and display functions on a Bell UH-1H helicopter. It is a simplex system which has the capability to satisfy a broad range of experiment requirements with several levels of sophistication. Three basic operational modes have been programmed into the digital computer and any one can be used with or without the flight director: manual, control stick steering (CSS), and AUTO. The system is capable of flying conventional autopilot modes and of providing waypoint guidance which provides radial guidance to an arbitrary waypoint selected by the pilot. Approaches can be made using either a standard instrument landing system (ILS) or the microwave landing system (MLS) with selective glide slopes and azimuth angles. Using MLS data, a helical descent can be made to hover and touchdown. The system also provides for capturing and tracking a preprogrammed three-dimensional reference flightpath.

HARDWARE

The hardware elements of the V/STOLAND system and their basic interconnections are shown in figure 1. They basically consist of displays; sensors; flight controls; two digital computers and their interface to the other system elements through a data adapter; a servo interlock unit which has the servo amplifier electronics and servo monitors in it; and the data acquisition system. The software program used for the acceptance tests and resident in the basic computer will be discussed in later sections.

The Sperry 1819B general purpose digital computer is an advanced version of the Sperry 1819A. It is a 16K, 18-bit word machine capable of many real-time operations in an airborne environment. The basic computer interfaces with the data adapter; the data adapter interfaces the computer to the rest of the system. The data adapter performs all of the analog-to-digital and digital-to-analog conversions, and digital-to-digital data transfers. The basic computer has the basic software program provided by Sperry. It was this basic program that was acceptance tested. The research computer, the second computer of the system, is the same type as the basic computer and is used for research software programs developed by the NASA and Army experimenters. These programs interface with and complement the basic software program. The research computer can

have its own navigation, guidance, or control laws, special filters or display functions, etc., which can be used without making any changes to the basic software program.

The displays (attitude director indicator (ADI), horizontal situation indicator (HSI), and multifunction display (MFD)) provide the inertial, navigation, and guidance information. The ADI has three cues, pitch and roll cyclic and collective, in addition to the basic attitude data. The MFD has a stroke written display that shows horizontal background data such as geographical features, NAVAID locations, and reference flightpaths. The control panels include the mode select panel for selecting the V/STOLAND system operating modes, the keyboard for entering selected gains into the computer, and an MFD control panel for selecting preprogrammed displays on the MFD and for engaging selected operating modes.

The flight sensors include rate gyros, vertical gyro, directional gyro, body-mounted longitudinal, lateral and vertical accelerometers, radio altimeter, low airspeed sensor (J-Tec VA 210), vibrating-diaphragm-type static pressure sensor, and an LTN-51 inertial navigation system (which was not used for the acceptance test flights). For navigation, the system has a VOR/LOC, DME, ILS, TACAN, and a prototype microwave landing system called MODILS.

The flight controls interfaced with the V/STOLAND system are noted in figure 1.

A servo interlock unit provides the interface for the V/STOLAND control commands and mode switches to engage and control the series and parallel servos for driving the aircraft controls.

The data acquisition system (DAS) records all flight data on an on-board analog magnetic tape recorder and simultaneously telemeters it to a ground station. The DAS interfaces with V/STOLAND via the data adapter as shown in figure 1; it also interfaces to some sensors directly. The data are recorded onboard and also telemetered to the ground in a pulse-code modulation (PCM) serial bit stream. The flight data consist of: (1) up to 80 digital variables from the V/STOLAND computers, (2) processed sensor data and servo commands from the servo interlock unit, and (3) direct inputs from other sensors on the aircraft. The digital variables from the computers are chosen by software in the 1819B computers. The ground data acquisition system receives the telemetered PCM data stream, merges it with radar position and velocity data, and then records it on a digital tape recorder and displays it in real-time on line printers, strip-chart recorders, x-y plotter, and CRT (cathode-ray-tube) monitors. The recorded data are used for post-flight analysis.

Photographs of the system installation are shown in figures 2 through 6. The figures show the air-cooled equipment rack which has an internal blower for mounted electronic units that require cooling, a non-air-cooled equipment rack where units that do not require cooling air are mounted, such as the navigation aids and data acquisition system, a true airspeed sensor (TAS) mounted on the front right side of the helicopter, cockpit displays, navigation radio controllers in the center console of the cockpit, and the INS platform for mounting the LTN-51 system and the rate gyros and accelerometers. The rate gyros and accelerometers were used as the prime inertial sensors by V/STOLAND during the acceptance tests. The vertical gyro (MD-1) and the gyromagnetic compass set (AN/ASN-43) used by V/STOLAND for attitude and heading references are the aircraft gyros mounted in the nose of the aircraft. The TAS sensor is a J-TEC VA 210 sensor capable of measuring true airspeed in the range from 0 to 200 knots. The flight-control installation in the UH-1H aircraft is shown in figure 7. There are four parallel and four series servos; one of each in each axis. The

parallel servos are electromechanical rate servos that have nearly full authority, but limited rate capability; they move the cyclic sticks and pedals. The series servos are electrohydraulic and have limited authorities: 26 percent in pitch, 29 percent in roll, 30 percent in yaw, and 19 percent in collective.

The left-side cyclic stick has pilot-controlled electrohydraulic disconnect links in the control system which allow the V/STOLAND system to be flown fly-by-wire in the control stick steering (CSS) mode. When not in the CSS mode, the pilot can reconnect the disconnect links in the roll and pitch axes and have a standard configured control system.

Flight-Control Augmentation System

The elements of the flight-control augmentation system are depicted in figure 1. The system consists of a limited authority simplex system of series actuators and parallel actuators, one of each in each of the four control linkages, pitch and roll cyclic, pedals, and collective. These servos are driven by the basic software in two modes of operation, the AUTO mode and the control stick steering (CSS) mode. The following discussion is presented in two parts: the actuator complex and control stick steering system.

Actuator complex– Figures 7(a), (b), and (c) show the servo installations for the cyclic, pedals, and collective controls. Also shown are the associated position and force sensors, and magnetic brakes which are interfaced with the control system software. These diagrams terminate at the vehicle's own boost actuators (not shown). Two additional items shown in figure 7(a) are the disconnect links for pitch and roll cyclic. These disconnects, which are not present in the other controls, provide a fly-by-wire capability for the research cyclic stick in the CSS mode. The research pedals and collective remain hard-linked to the controls at all times and augmentation in the CSS mode is derived primarily through the limited authority series actuators.

Table 1 lists the characteristics of the servos, including the boost, and figure 8 shows an analog representation of how those servos are interconnected with one another. The series actuator, which is driven as a position servo, has a high-frequency response of greater than 10 Hz. The parallel actuator, which is driven as a rate servo, has much lower response characteristics. The boost actuator is the standard UH-1H position servo with a frequency response slightly less than 10 Hz. The parallel actuator serves as a trim servo that drives to null to "off-load" the series servo.

During the AUTO mode, the series and parallel servos are driven continuously by control laws generated in the computer. The disconnect links in the cyclic stick are left engaged (hard-linked) and thus both pilots can monitor the control activities of parallel actuators through the motions imparted to the controllers. In the CSS mode the disconnect links are disengaged (soft-link) and again the series and parallel actuators are driven continuously. However, in the pedals and collective, the parallel actuator must be inhibited while the pilot is making inputs, otherwise a force coupling back to the pilot would occur. Disablement of the collective parallel actuator is achieved via a trigger on the collective grip and through force sensing on the pedals parallel actuator.

Of particular concern with a control system of this type are the effects, from a safety standpoint, of a hardover failure of one or more actuators in flight. To this end, a considerable amount of ground simulation was conducted followed by a single axis hardover failure study in

flight at both 60 knots and at hover. Tables 2 and 3 show the maximum excursions resulting from each of the single axis failures. More details of this failure study may be found in reference 2. Although the comparison between simulation and flight is, in general, good, the excursions for flight tended to be less. This may be due in part to the procedure by which the failures were introduced. In flight, the pilot had prior knowledge of the initiation of a failure but in the simulator tests the failures were unannounced. As a result of those tests it was concluded that none of the single axis failures presented a major problem to the recovery task.

Control stick steering– The control stick steering (CSS) mode is the piloted augmented flight control mode that resides in the software of the basic computer. This mode consists of a prefilter, model-following type of control in the cyclic and collective controls and a response-feedback type of control for the pedals. The pitch and roll response is governed by a second-order attitude command with a natural frequency of 3 rad/sec and the height response by a first-order rate command with a time constant of 0.5 sec. The expressions for these models and for the yaw response feedback control are given below.

1. Pitch

$$\theta_c' = \frac{3^2 K_{\delta_\theta} \delta_\theta}{S^2 + 1.4(3)S + 3^2}$$

2. Roll

$$\theta_c' = \frac{3^2 K_{\delta_\phi} \delta_\phi}{S^2 + 1.4(3)S + 3^2}$$

3. Height

$$\dot{h}_c' = \frac{2K_{COL}\delta_{COL}}{S + 2}$$

4. Yaw

$$\psi_c = \text{heading hold command}$$

$$r_c = K_{FPH} F(F_{FP}, F_{FPO})$$

For completeness, many of the above expressions are synchronized and trimmed by terms that are not shown. Such terms are needed for smooth engagements into CSS and for trimming but do not affect the basic model responses. Those terms will not be discussed here but further details may be found in reference 3. For purposes here the synchronized and trimmed versions of θ_c', ϕ_c', and $\dot{h}_c'$ will be referred to as θ_c, ϕ_c, and $\dot{h}_c$, respectively.

A second portion of the flight-control software contains the actuator commands or control law equations. Those command equations, which are used by both the CSS and AUTO modes, are listed below.

1. Pitch actuator commands

Series

$$B_{SS} = K_{\delta_{\theta FF}}\left(\frac{S}{S+10}\right)\delta_\theta + K_{BFF}\left(\frac{S}{S+8}\right)\theta_c - K_q\left(\frac{S}{S+0.167}\right)q + K_\theta(\theta_c - \theta)$$

where $K_{\delta_{\theta FF}} = 0$ in AUTO mode.

Parallel

$$B_{PS} = K_{BPS}B_{SS}$$

2. Roll actuator commands

Series

$$A_{SS} = K_{\delta_{\phi FF}}\left(\frac{S}{S+10}\right)\delta_\phi + K_{AFF}\left(\frac{S}{S+6}\right)\phi_c - K_p p + K_\phi(\phi_c - \phi)$$

where $K_{\delta_{\phi FF}} = 0$ in AUTO mode.

Parallel

$$A_{PS} = K_{APS}A_{SS}$$

3. Height actuator commands

Series

$$C_{SS} = -K_{\ddot{h}}\left(\frac{S}{S+0.167}\right)\ddot{h} + K_{\dot{h}}(\dot{h}_c - \dot{h})$$

Parallel

$$C_{PS} = K_{CPS}C_{SS}$$ (disabled when C-button on collective grip is pressed)

4. Yaw actuator commands

Series – at hover

$$D_{SS} = K_{FDC}\left(\frac{S}{S+1}\right)\theta_{COL} + K_r(r - r_c) + K_\psi(\psi - \psi_c)$$

Series – at cruise

$$D_{SS} = K_{FDC}\left(\frac{S}{S+1}\right)\theta_{COL} + K_r r_{wo} - K_{DP}\left(\frac{2}{S+2}\right)p + K_{ay}\left(\frac{1}{S+1}\right)a_y$$

where

$$r_{wo} = \frac{S}{S+0.1}\left(r - \frac{1845}{V_G}\sin\phi\right)$$

(The transition between hover and cruise occurs at V_{Ht} = 25 knots, where V_{Ht} equals the true airspeed V_t when the height (h) above the runway is greater than 40 ft; it equals the ground speed V_G when h is below 20 ft; and it is a linear blend of V_G and V_t between 20 and 40 ft. The command DSS is synchronized across the transition to prevent transients.)

Parallel

$$D_{PS} = K_{DPS}D_{SS} \text{ (disabled when pedal force } F_{FP} > F_{FPO})$$

The rationale for these control equations is largely based on the contractor's experience with helicopter stabilization systems. No particular gain optimization procedure was employed for the selection of these signs but rather a perturbation about the values used for similar systems was the main technique used. The original gains used at the start of the flight acceptance tests and the final values arrived at by the end of the tests are shown in table 4.

It is of course desirable to maintain these control gains (particularly K_θ, K_ϕ, K_h) as high as is practicable so as to increase the system bandwidth and improve the fidelity with which the vehicle can respond to the CSS and AUTO equations. In flight, however, it was found that certain frequencies in the 2- to 10-Hz range were excited by the system and thus some of the final gains on table 4 represent significant reductions from those found appropriate on the simulator. Both low-pass and notch filtering were employed to minimize the effects of these structural and rotor frequencies; however, such filtering also restricts the magnitude of the control gains that can be used and also results in poorer model following.

Guidance System

The guidance system can be divided into two sections, nonlanding and landing modes. In each case, the guidance modes compute commands that are applied to the stability and control system. The control system converts bank angle commands into lateral cyclic servo commands, pitch attitude commands into pitch cyclic servo commands, and altitude rate commands into collective servo commands.

Nonlanding modes– The nonlanding guidance modes are designed to be used in the climb, cruise, and descent phases of flight. They are described below.

The flightpath angle select and hold mode generates an altitude rate command to fly the aircraft at a constant, air-referenced, flightpath angle. The select feature allows the pilot to change the commanded angle from the mode select panel.

The altitude select and hold mode generates an altitude rate command to fly the aircraft at a constant barometric altitude. The altitude select mode allows the pilot to change the commanded altitude through the mode select panel. When a change is entered, an appropriate flight path is computed and the aircraft is commanded to climb or descend at that angle until the commanded altitude is reached; the system then reverts to the altitude hold mode.

The airspeed select and hold mode generates a pitch attitude command to fly the aircraft at a commanded airspeed. The commanded airspeed can be changed at any time through the mode select panel.

The heading select mode generates a bank angle command to fly the aircraft to the selected magnetic heading. The heading command can be changed through the mode select panel. Heading hold is automatically selected when either the flight director or autopilot modes are selected unless the helicopter is in a turn exceeding a 5° bank angle.

The TACAN or VOR/DME course modes allow the pilot to track a TACAN or VOR radial. These modes generate bank angle commands proportional to angular error from the desired radial.

Landing modes– The landing modes are designed for the terminal area reference flight paths, final approach for landing using a helix or a straight-in approach, hover, and letdown.

The landing guidance includes the computation of the reference flightpath (RFP) shown in figure 9. The path is composed of straight and circular segments connecting seven waypoints referenced to the runway coordinate system. The final segment of the RFP between waypoints 6 and 7 is determined by the type of approach selected. The straight-in approach, shown in figure 10, follows the runway centerline extension in the horizontal plane and follows the selected microwave landing system (MLS) glide slope in the vertical plane. The MLS glide slope intercepts the ground plane short of the touchdown point. The MLS used for these flight tests was a prototype time reference scanning beam system designated MODILS. The accuracies are: azimuth, ±0.25°; elevation, ±0.07°; and range, ±0.01 mile.

The helix approach shown in figure 11, consists of a spiral descent around a cylinder of radius 1160 ft with a glide slope of 6.11°. At the end of the helix, the RFP continues along the 6.11° glide slope until the final flare point.

The final flare and letdown segments of the RFP are the same for either a straight-in or a helix approach. As shown in figure 10, the path follows the descent glide slope of MLS glide slope until it intercepts a 2.5° glide slope originating at the touchdown point. The 2.5° glide slope segment was selected for the development stages of system testing in order to avoid operating the single-engine helicopter in the unsafe areas of the height-velocity curve. At a height of 10 ft above the ground, the aircraft levels off and hovers above the touchdown point where the letdown to landing is performed.

For either a helix or a straight-in approach, the pilot maneuvers the aircraft manually or automatically with the nonlanding modes, to intercept the RFP prior to where the helix or straight-in glide slope begins. The guidance system generates a bank angle command, proportional to cross-track displacement and rate errors, and generates an altitude rate command proportional to

vertical displacement errors to keep the aircraft on the RFP. It generates a pitch command in response to airspeed errors.

During the flare to hover, the guidance system generates a pitch command proportional to ground speed errors from a variable ground speed reference that is a function of distance to the touchdown point. Using MLS navigation, the aircraft is commanded to perform a decrab maneuver when the hover conditions are met, which aligns the aircraft heading with the runway at a 12-sec time constant. In the flight director land modes, this maneuver cannot be commanded by the guidance system because there is no flight director cue for the pedals; the pilot must use his judgment in manually controlling heading. When the system determines that the aircraft is 10 ft over the touchdown point and stabilized with an estimated longitudinal ground velocity of less than 0.5 ft/sec, and the longitudinal and position errors less than 48 ft, it initiates the letdown mode. Then, the altitude rate is commanded as a function of altitude so that the aircraft touches down with a sink rate less than 0.2 ft/sec. At touchdown, the system is disengaged by feelers on the skids or manually by the pilot.

Navigation System

The navigation system provides the aircraft position and velocity estimates for the guidance system to compute the guidance commands. It converts the various radio navigation-aid measurements into runway coordinate system components and combines them with strap-down accelerometer measurements and airspeed measurements in complementary filters to provide smoothed position and velocity estimates. The navigation aids used are determined by the location of the aircraft in the terminal area. Outside the coverage of the MLS, the navigation is based on either TACAN or VOR/DME along with barometric altitude measurements. Inside MLS coverage, the navigation is based on MLS azimuth, elevation, and range measurements. The navigation aids may be selected either manually or automatically depending on pilot preference and NAVAID availability.

FLIGHT-TEST RESULTS

Control System Performance

The control system performance was assessed by step and sinusoidal responses in the simulation and by step responses in flight. The criterion for acceptable performance was based on the error between a commanded and measured response. For 2.5-cm (1-in.) steps in pitch or roll, this criterion was set at a maximum error of 35% between θ_c and θ or ϕ_c and ϕ for the first 1-sec period and at 10% thereafter. These percentages were based on the steady-state attitudes. In the case of collective response the criterion was 20% error between $\dot{h}$ and $\dot{h}_c$ in the first 1-sec period and at 10% thereafter. In addition, all step responses should exhibit the well-damped characteristics of the models described earlier. The initial V/STOLAND development requirements were keyed to a system for navigation and guidance research and not for control law investigations. Consequently, these criteria represent a rather lax requirement and were not to be considered indicative of what is necessary for good model-following control system response.

Figures 12 show the simulation 1-in. step responses for 60 knots utilizing the original gains shown on table 2. These responses are well damped in pitch and roll but exhibit an oscillatory tendency in the collective response. Relative to the criterion above, only pitch was out of tolerance with a 40% error in the first 1-sec period. The step responses for hover exhibited a similar behavior and are not shown here. Although these responses do not represent a good model following, the CSS system was found to be generally acceptable for the approach tasks performed on the simulator.

The flight step responses are shown in figures 13. These responses are for a flight condition of 60 knots and represent the CSS response for the final gains given on table 2. These final gains were, in many cases, significantly smaller than the original gains and were an attempt to eliminate the oscillations that occurred when the original gains were first tried in flight. Such oscillations were apparently due to modes of unidentified origin that were neither modeled in the simulation nor in the analytical design of the control equations.

As can be seen by the responses in figure 13(a) the reduced gains for pitch yielded a response which was very similar to the simulator response of figure 12(a). However, the roll response shown in figure 13(b) was oscillatory and also was accompanied by a limit cycling of the series actuator (A_{SS}). Since this situation prevailed at the close of the contract, acceptance for this portion of the system consisted of a hardware acceptance only and the CSS system was delivered in an unflyable status.

One final assessment which shows the limitations of the CSS system response is shown in figure 14. This figure shows the closed-loop frequency response of the pitch and roll control as measured in the simulator with the original gains and as calculated for the final gains. The calculated frequency responses utilized greatly simplified models of UH-1H pitch and roll dynamics consisting of first-order fits to unaugmented step responses from flight data. These models are:

Pitch

$$4.75\, B_{IS} = S(S + 0.5)\theta$$

Roll

$$7.5\, A_{IS} = S(S + 3)\phi$$

When combining these expressions with the command equations and the simplified actuator equations as shown below,

Pitch command

$$B_{SS} = (-0.45S - 0.6)\theta + \left(0.375S\,\frac{8}{S+8} + 0.6\right)\theta_c$$

Roll command

$$A_{SS} = (-0.212S - 0.5)\phi + \left(0.375S\,\frac{6}{S+6} + 0.5\right)\phi_c$$

Actuator (pitch)

$$B_{IS} \cong \left(1 + \frac{0.75}{S}\right) B_{SS}$$

Actuator (roll)

$$A_{IS} \cong \left(1 + \frac{0.125}{S}\right) A_{SS}$$

The following closed-loop transfer functions result and were the basis for the calculated gain and phase plots shown in figure 14:

$$\frac{\theta}{\theta_c} = \frac{1.78(S^2 + 2.35S + 1.20)}{(S + 0.7)(S^2 + 1.94S + 3.04)}$$

$$\text{dc gain} = \frac{(1.78)(1.20)}{(0.7)(3.04)} \cong 1$$

$$\frac{\phi}{\phi_c} = \frac{2.81(S^2 + 1.46S + 0.17)}{(S + 9.5)(S^2 + 3.64S + 0.5)}$$

$$\text{dc gain} = \frac{(2.81)(0.17)}{(0.95)(0.5)} \cong 1$$

It can be seen that in the frequency region of the attitude model for the CSS system (i.e., $\omega = 3$) the calculated responses and the simulator pitch response yielded phase lags in excess of 45°. Only the simulator roll response showed an acceptable phase plot. The influence of these lags has already been demonstrated by the step response.

Midway in the program the gain terms $K_{\delta_{\theta FF}}$ and $K_{\delta_{\phi FF}}$ were added to provide lead and to help improve the model-following fidelity of the CSS mode. These terms have not yet been fully exploited. It is expected that with the use of such lead terms and with the utilization of different filter techniques, such as described in reference 4, that an increase in the model-following bandwidth can be achieved. This, coupled with a more rigorous procedure for selecting the control gains, will be necessary to provide a versatile in-flight simulation capability through model following.

Guidance System Performance

The guidance system performance was assessed first in the simulation and then in actual flight. The criteria for acceptable performance were based on the system operating with specified guidance errors and operating per the technical specifications of the contract in which the system was procured. The system was fully tested in the simulation; it included testing the automatic modes, flight director modes, and also the failure monitors by inserting system failures and off nominal flight conditions.

In cases where the guidance performance did not meet the acceptable requirements and the validity of the aircraft model in the simulation could have been a factor, the performance was conditionally passed depending on its performance in flight.

Flight-test results and typical time history plots of the responses are discussed below.

Flightpath angle select/hold– Upon flightpath angle (FPA) selection using the mode select panel, the climbs or descents were entered automatically by collective control input with directional and cyclic control inputs to counter coupling. Heading was maintained precisely during these profiles and true airspeed errors produced some cyclic pitch activity and airspeed variations.

Figure 15 shows the commands and responses for flightpath angle (γ), pitch attitude (θ), and true airspeed (V_T) over a 300-sec interval. The FPA select mode was engaged at about 25 sec (on the graph) and the selected +7.5° flightpath angle reference was captured at about 30+ sec, engaging the FPA hold mode. Subsequent FPA select/hold modes were engaged for 0°, -7°, and +7°, respectively. The final negative FPA select mode was disengaged at about 290 sec when altitude hold was engaged. The bottom graph of figure 15 shows the commanded true airspeed (V_{CF}) of 60 knots, and the actual true airspeed (V_T).

Figure 15 shows how the pitch attitude command essentially follows the true airspeed error (but is modified by a rate-limited lag filter plus an integral component of the velocity error). It also shows the resulting pitch attitude.

Altitude select/hold– Figure 16 shows performance during altitude select and hold conditions over a 200-sec period. At the start of the graph the FPA mode is engaged as an automatic submode when altitude select is armed. Altitude select engages at about 63 sec and altitude hold engages at about 70 sec. During this mode of operation, pitch attitude varied with true airspeed error to a lesser degree than during FPA modes. The excessive h variation followed the collective pitch activity (not shown in the figure) and was not acceptable; it must be improved. For all of this control activity, the altitude variation was negligible. At approximately 110 sec, altitude select is armed, engaging a negative flightpath angle, with capture and hold performance similar to the previous case.

Heading select/hold– Figure 17 illustrates heading select/hold performance, first for a 90° right turn, then back again to the original heading. The roll attitude command (ϕ_C) is limited to 20° in this mode.

With heading hold and altitude hold engaged, headings of about 90° right and left of course were selected. The helicopter rolled smoothly into the turns and maintained coordinated flight while turning. Smooth rollouts on selected headings were performed and the system reverted to heading hold upon completion of each turn. The system worked harder to maintain altitude in right turns compared with those to the left, as evidenced by increased collective pitch activity (not shown).

TACAN capture– Figure 18 shows the computed cross-track displacement and rate (D_Y and $\dot{D}_Y$) relative to a 330° TACAN radial. Capture is from the right side, and roll attitude (ϕ) is initially positive as is shown, being commanded by $D_Y + \tau\dot{D}_Y$ (τ varies from 20 to 10 sec as a function of

D_Y). Roll attitude then reverses to oppose a slight overshoot. The mode is disengaged at about 100 sec on the graph.

Figure 19 shows the same capture in an $x - y$ plot where x and y are the computed navigation estimates of the aircraft position in the aircraft coordinate frame. Figure 20 shows a similar $x - y$ plot based on the radar estimates of aircraft position.

VOR capture– Figures 21 through 23 show similar plots of the capture of a radial from the VOR station located at Stockton. However, since this station is about 25 n. mi. away, navigation accuracy was considerably degraded due to the 0.1° resolution of the VOR.

Reference flightpath– Figure 24 is an $x - y$ plot, based on computed navigation data, of a flight around the reference flightpath (fig. 9). The path is entered from the east side, as shown, and lateral capture occurs near (0,0) in the $x - y$ frame. For the first part of the path the navigation is based on TACAN data. About halfway down the west-side straight segment the MODILS navigation data becomes valid, and the navigation computations automatically transition to this new more accurate reference. Any difference between the two references induces a transient in the position estimation, as is shown. Note that the plot shows estimated position, not actual. The aircraft will also experience a transient, but not as severe as that shown in the plot.

Straight-in land, 7.5° glide slope– Figures 25 through 27 illustrate automatic straight-in landing to touchdown where the initial glide slope is 7.5°. The time scale in figures 26 and 27 is quite compressed to accommodate the 5-min trajectory on the graph. Interception of the straight-in approach path was made with a 45° right turn to on-course. A small overshoot occurred which was corrected within 15 sec. Precise lateral tracking was noted for the approach as illustrated in figure 26. The 7.5° glide slope was captured at approximately 110 sec (fig. 27) and tracked until interception of the 2.5° segment at approximately 230 sec. During the approach, some pitch oscillation was evident along with true airspeed (V_T) variations as shown in figures 26 and 27.

The flare began at about 250 sec (see fig. 27) at which time the velocity control loop started controlling ground speed (V_G – not plotted) instead of V_T. The velocity command V_{CF} therefore made a step change reflecting the difference between V_G and V_T.

Figure 25 shows the $x - y$ plot of the landing trajectory, based on computed navigation data.

Straight-in land, 10° glide slope– Figures 28 through 30 are analogous to the three previous figures except for a 10° glide slope. The higher rate of descent (about 850 ft/min at 60 knots) is shown on the h plot of figure 30.

Straight-in land, 12.5° glide slope– Figures 31 through 33 are also analogous to the previous two sets of figures, and illustrate the performance obtained with a 12.5° glide slope. The rate of descent was about 1000 ft/min.

Helix land– Figures 34 through 36 illustrate flight performance for a helix-land sequence. The aircraft captured the initial straight segment of the helix-land trajectory from the left side as is shown in the $x - y$ plot in figure 34, and in the D_Y plot in figure 35. The helical segment was captured at about 130 sec and the aircraft rolled into about a 15° banked turn and started descending on a 6° glide slope, as is shown. The jumps in D_Y and D_Y occurred when the lateral

reference changed from a straight to a circular segment at a point prior to the point of tangency. (The jumps in Dy and Dy are in opposite direction and complement each other to produce a smooth roll command.) The exit from the helical segment can be seen on the Dy and Dy plots at approximately 330 sec.

Figure 36 shows some longitudinal pitch oscillation and collective activity during the spiral approach, which is similar to that encountered during the straight-in approaches.

Letdown mode– The estimated ground velocity often exceeded the 0.5 ft/sec threshold criterion for letdown when the aircraft was actually stationary, preventing the letdown mode from engaging for excessive periods of time. Additional effort will be necessary to improve the ground velocity and position estimates near the touchdown point. The resolution of the MODILS navigation system was 0.01 n. mi. in range and 0.1° in azimuth, which limited precision landings. The landing dispersion distances about the designated touchdown point were within 50 ft laterally in the y direction and 65 ft longitudinally in the x direction. The letdown rate was less the 0.2 ft/sec at touchdown.

CONCLUSIONS

All functions of the V/STOLAND system were demonstrated in both a fixed-based simulator at NASA/ARC and in flight. All of the pilot assists modes and automatic guidance on programmed reference flightpaths were successfully tested. Fully automatic approaches to touchdown were made with various glide slopes with straight-in and three-revolution helical approaches. The approaches were acceptable, but the hover and letdown performance was not acceptable due to a problem the system had in estimating position and ground velocity from the MODILS data. More development will be needed on this by the Government after acceptance from the contractor. Touchdown dispersions during automatic landings were within 65 ft of the aim point in the x and y directions; the specifications required the touchdown dispersions to be within 50 ft.

The control stick steering mode, fly-by-wire, which has pilot input control on the cyclic pitch and roll, and automatic control on the collective and yaw, was tested. Control gains had to be reduced and filtering added to the three-rate gyro signals to maintain control stability with the structural and rotor vibrations. The resultant bandwidth obtainable for altitude control was sufficient for guidance but poor for model following control systems. The original design objectives of the system, however, were primarily for guidance and navigation and not for model-following control system investigations.

The flight director worked reasonably well in the cruise and approach modes; however, some optimization will be required for full pilot acceptance. Because the system was not designed with a flight director cue for pedals, the decrab maneuver near hover and the heading-hold at hover cannot be commanded by the guidance system. The pilot is required to use his judgment in manually controlling heading with the pedals without a flight director cue.

Ames Research Center
National Aeronautics and Space Administration
Moffett Field, California 94035, July 25, 1979

REFERENCES

1. Liden, S.: V/STOLAND Digital Avionics System for UH-1H. Final Report, NASA CR-152179, 1978.

2. Corliss, Lloyd D.; and Talbot, Peter D.: A Failure Effects Simulation of a Low Authority Flight Control Augmentation System on a UH-1H Helicopter. NASA TM-73,258, 1977.

3. Liden, S.: V/STOLAND Control Stick Steering Specification and Program. Sperry Report 5440-0888-P01, Sperry Flight Systems Division, Phoenix, Arizona, NASA contract NAS2-7306, 1978.

4. Garren, J. F.; Niessen, F. R.; Abbott, T. S.; and Yenry, K. R.: Application of a Modified Complementary Filtering Technique For Increased Aircraft Control System Frequency Bandwidth in High Vibration Environment. NASA TM X-74004, 1977.

TABLE 1.– ACTUATOR CHARACTERISTICS

Axis	Authority, %	Dynamics	Rate limits, deg/sec
Roll			
Series	29	ω_o = 75 rad/sec; ζ = 0.7	±20
Parallel	≅100	$1/\tau$ = 40 rad/sec	±2.8
Boost	100	$1/\tau$ = 50 rad/sec	±20
Pitch			
Series	26	ω_o = 75 rad/sec; ζ = 0.7	±20
Parallel	≅100	$1/\tau$ = 40 rad/sec	±2.8
Boost	100	$1/\tau$ = 50 rad/sec	±20
Yaw			
Series	30	ω_o = 75 rad/sec; ζ = 0.7	±20
Parallel	≅100	$1/\tau$ = 40 rad/sec	±2.8
Boost	100	$1/\tau$ = 50 rad/sec	±20
Collective			
Series	19	ω_o = 75 rad/sec; ζ = 0.7	±20
Parallel	≅100	$1/\tau$ = 40 rad/sec	±2.8
Boost	100	$1/\tau$ = 50 rad/sec	±20

TABLE 2.– HARDOVER DATA AT HOVER

Failure	θ, deg	ϕ, deg	ΔX		ΔY		Height loss		Pilot reaction, sec	Rotor flapping, deg	Number of runs
			ft	m	ft	m	ft	m			
(a) Simulation											
Pitch down	$\frac{22}{10}$ 15	$\frac{13}{2}$ 7	$\frac{35}{15}$ 25	$\frac{10.6}{4.6}$ 7.6	$\frac{40}{0}$ 20	$\frac{12.2}{0}$ 6.1	$\frac{30}{0}$ 10	$\frac{9.1}{0}$ 3	$\frac{1}{0.25}$ 0.55	4.5	9
Pitch up	$\frac{32}{4}$ 19	$\frac{19}{12}$ 14	$\frac{100}{25}$ 62	$\frac{30.5}{7.6}$ 18.9	$\frac{20}{10}$ 15	$\frac{6.1}{3}$ 4.6	$\frac{90}{0}$ 61	$\frac{27.4}{0}$ 18.8	$\frac{1}{0.25}$ 0.55	4.5	6
Coll. down	$\frac{12}{0}$ 5	$\frac{7}{0}$ 4	$\frac{60}{10}$ 35	$\frac{18.3}{3}$ 10.6	15	4.6	$\frac{60}{0}$ 35	$\frac{18.3}{0}$ 10.6	$\frac{2}{0.5}$ 1.3	3	10
Coll. up	$\frac{11}{2}$ 5	$\frac{11}{2}$ 7	15	4.6	$\frac{10}{5}$ 7.5	$\frac{3}{1.5}$ 2.2	0	0	$\frac{1.5}{0.5}$ 1.0	4	6
Roll right	$\frac{15}{5}$ 11	$\frac{29}{12}$ 22	$\frac{40}{10}$ 25	$\frac{12.2}{3}$ 7.6	$\frac{60}{35}$ 48	$\frac{18.3}{10.6}$ 14.6	$\frac{15}{0}$ 2	$\frac{4.6}{0}$ 0.6	$\frac{1}{0.5}$ 0.55	4.5	10
Roll left	$\frac{15}{4}$ 8	$\frac{30}{10}$ 22	$\frac{35}{20}$ 27	$\frac{10.6}{6.1}$ 8.2	80	24.4	$\frac{20}{0}$ 8	$\frac{6.1}{0}$ 2.4	$\frac{1.5}{0.2}$ 0.7	5.5	8
Yaw right	$\frac{9}{2}$ 5	$\frac{10}{2}$ 5	$\frac{35}{5}$ 20	$\frac{10.6}{1.5}$ 6.1	$\frac{50}{15}$ 30	$\frac{15.2}{4.6}$ 9.1	$\frac{40}{0}$ 11	$\frac{12.2}{0}$ 3.4	$\frac{1.5}{0.5}$ 1	4	8
Yaw left	$\frac{6}{0}$ 4	$\frac{12}{2}$ 6	$\frac{30}{25}$ 27	$\frac{9.1}{7.6}$ 8.2	$\frac{50}{15}$ 30	$\frac{15.2}{4.5}$ 9.1	$\frac{16}{0}$ 2	$\frac{4.9}{0}$ 0.6	$\frac{0.75}{0.3}$ 0.6	3	13
(b) Flight											
Pitch down	11.5	5					5	1.5		3.6	
Pitch up	10	8.5					2	0.6		5.3	
Coll. down	9	9					14	4.3		2.4	
Coll. up	10	5					0	0		2.8	
Roll right	8	18.5					0	0		3.5	
Roll left	11	11.5					0	0		7.2	
Yaw right	9	6					0	0		2.5	
Yaw left	7	6					0	0		2.0	

Key: $\frac{22}{10}$ 15 — Largest maximum value; Averaged value; Smallest maximum value

TABLE 3.– HARDOVER DATA AT 60 KNOTS

Failure	θ, deg	ϕ, deg	ΔY		ΔY		Height loss		Pilot reaction, sec	Rotor flapping, deg	Number of runs
			ft	m	ft	m	ft	m			
(a) Simulation											
Pitch down	16/4 10	16/3 9			80/10 40	24.4/3 12.2	48/0 15	14.6/0 4.6	1.5/0.1 0.5	7.2	12
Pitch up	35/1 15	18/2 13			—	—	10/0 2	3/0 0.6	0.75/0.5 0.6	—	5
Coll. down	16/5 10	23/5 11			75/40 58	22.8/12.2 17.6	100/0 40	30.5/0 12.2	2/0.5 1.2	7.3	9
Coll. up	22/2 8	27/2 11			250/20 100	76.2/6.1 30.5	30/0 2	9.1/0 0.6	2.5/0.5 1.3	8	15
Roll right	18/4 10	27/15 19			160/40 100	48.7/12.2 30.5	20/0 5	6.1/0 1.5	0.75/0.5 0.4	8	8
Roll left	12/4 8	40/15 24			210/40 102	64/12.2 31	90/0 18	27.4/0 5.5	1/0.25 0.7	8	13
Yaw right	14/3 7	14/4 10			—	—	60/0 20	18.3/0 6.1	0.75/0.3 0.6	—	5
Yaw left	12/0 5	31/2 9			40/12 24	12.2/3.7 7.3	25/0 3	7.6/0 0.9	1.25/0.5 0.8	5	9
(b) Flight											
Pitch down	8	3					16	4.9		4.2	
Pitch up	9.5	5					0	0		5.1	
Coll. down	2	3					28	8.5		2.3	
Coll. up	3	6					0	0		3.2	
Roll right	3	18					0	0		4.4	
Roll left	2	23					—	—		5.1	
Yaw right	1	11					—	—		2.9	
Yaw left	2	8					—	—		3.1	

TABLE 4

Gain	Description	Original	Final	Units
K_{AFF}	Roll rate feed forward	3	2.25	deg/deg
K_{APS}	Roll parallel servo	0.5	0.125	deg/sec/deg
K_{BFF}	Pitch rate feed forward	3.0	3.0	deg/deg
K_{BPS}	Pitch parallel servo	1.0	0.75	deg/sec/deg
K_{COL}	Collective sensitivity	10	10	ft/sec/in.
K_{CPS}	Collective parallel servo	3.2	1.6	deg/sec/deg
K_{FDC}	Yaw/collective coupling	2.0	1.0	deg/deg
K_{DPS}	Directional parallel servo	0.4	0.4	deg/sec/deg
K_{DP}	Yaw/roll coupling	0.1	0.1	deg/deg/sec
K_{FPH}	Pedal sensitivity	2.0	1.0	deg/sec/lb
K_{ay}	Y body acceleration	2.0	2.0	deg/ft/sec^2
$K_{\dot{h}}$	Altitude rate	0.25	0.1875	deg/ft/sec
$K_{\ddot{h}}$	Altitude accelerometer	0.05	0.025	deg/ft/sec^2
K_p	Roll rate	0.425	0.212	deg/deg/sec
K_q	Pitch rate	1.5	0.45	deg/deg/sec
K_r	Yaw rate	0.6	0.6	deg/deg/sec
K_{δ_θ}	Pitch sensitivity	4	4	deg
$K_{\delta_{\theta FF}}$	Stick feed forward	—	1.35	deg
K_{δ_ϕ}	Roll sensitivity	8	8	deg/in.
$K_{\delta_{\phi FF}}$	Stick feed forward	—	0	deg/in.
K_θ	Pitch attitude	2.0	0.6	deg/deg
K_ϕ	Roll attitude	1.0	0.5	deg/deg
K_ψ	Heading	1.0	1.0	deg/deg

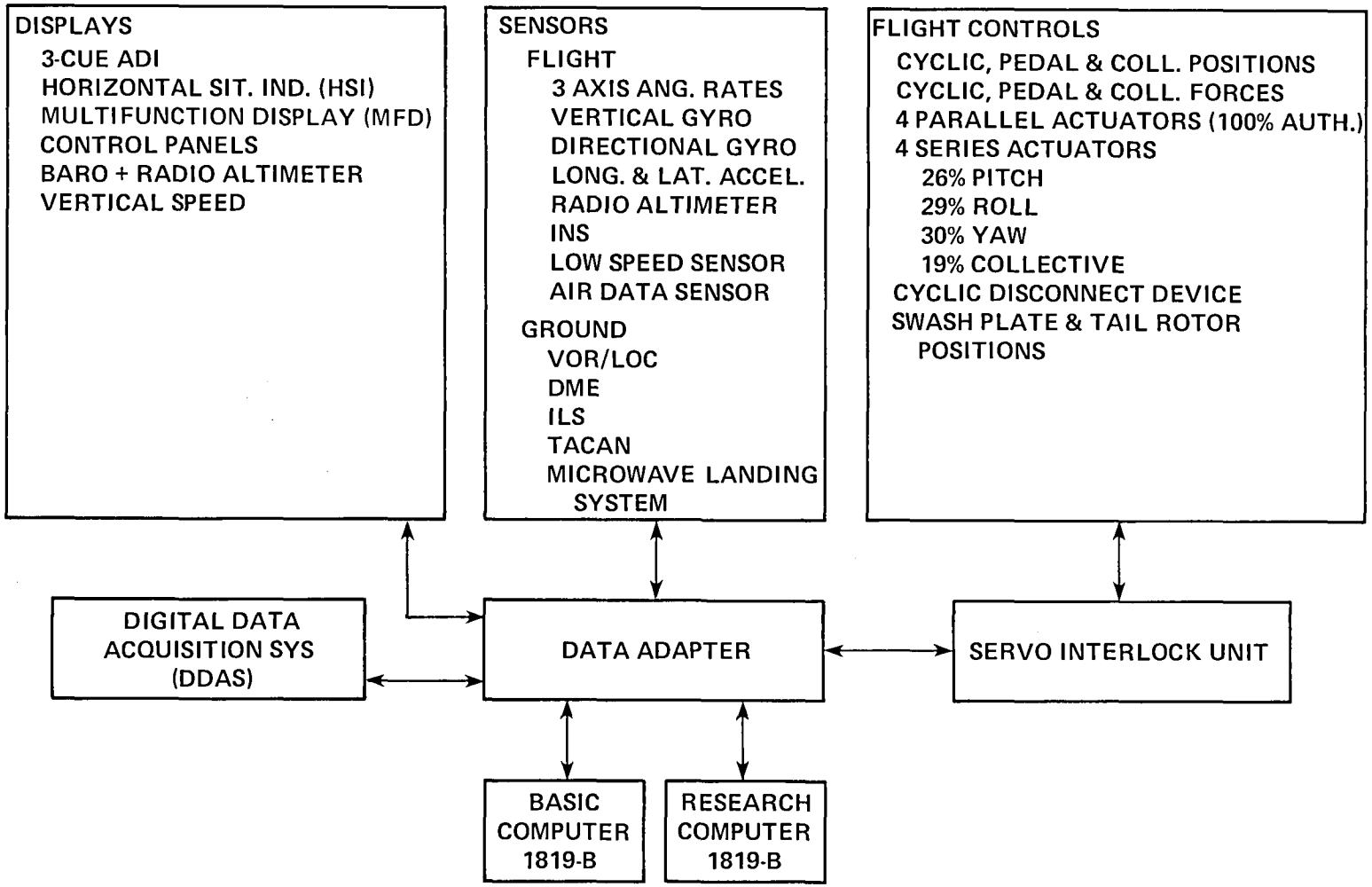

Figure 1.– Elements of the V/STOLAND system.

Figure 2.– Installation of the air-cooled equipment flight rack.

Figure 3.– Installation of the non-air-cooled equipment flight rack.

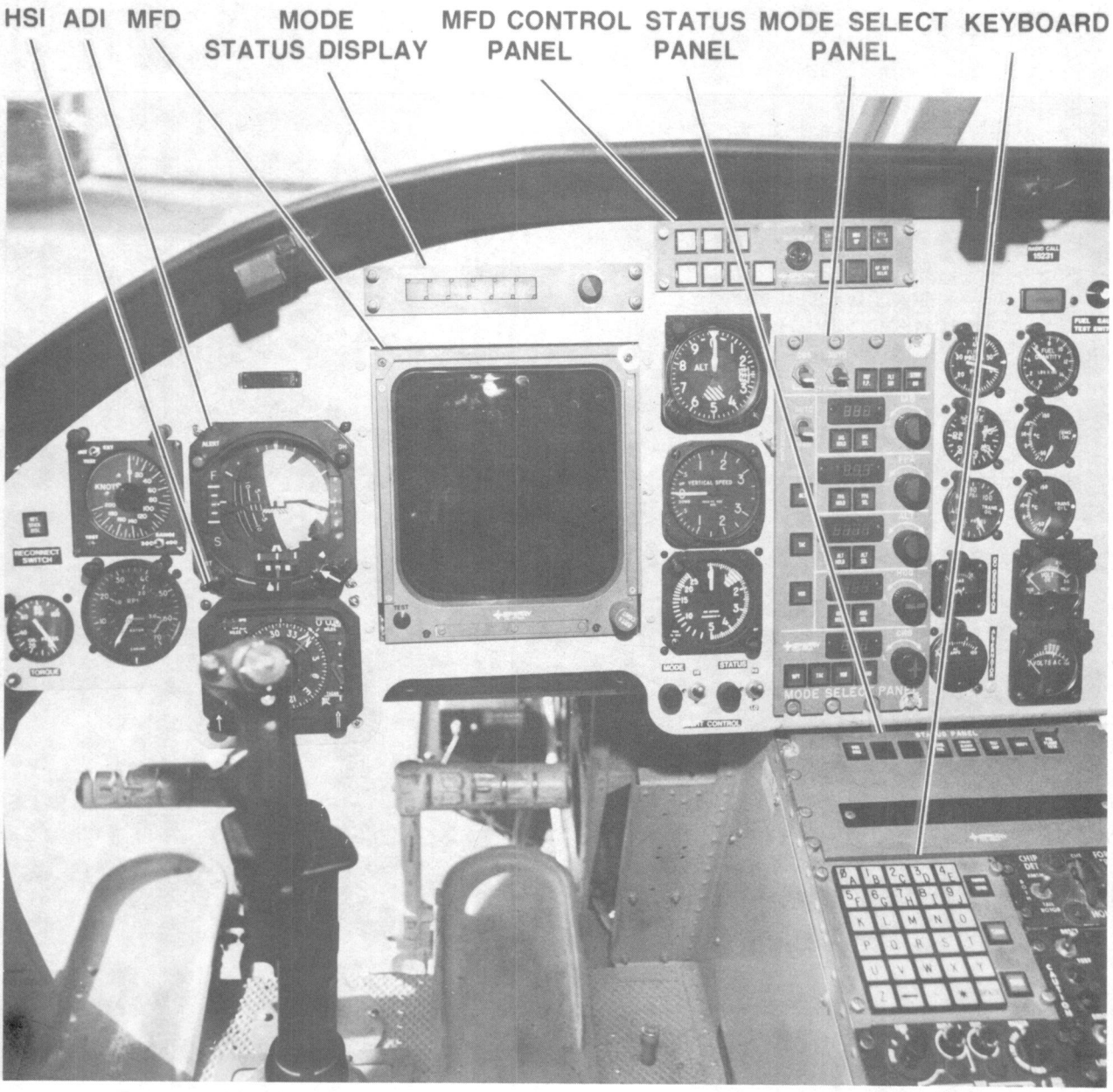

Figure 4.– Research pilot's instrumentation.

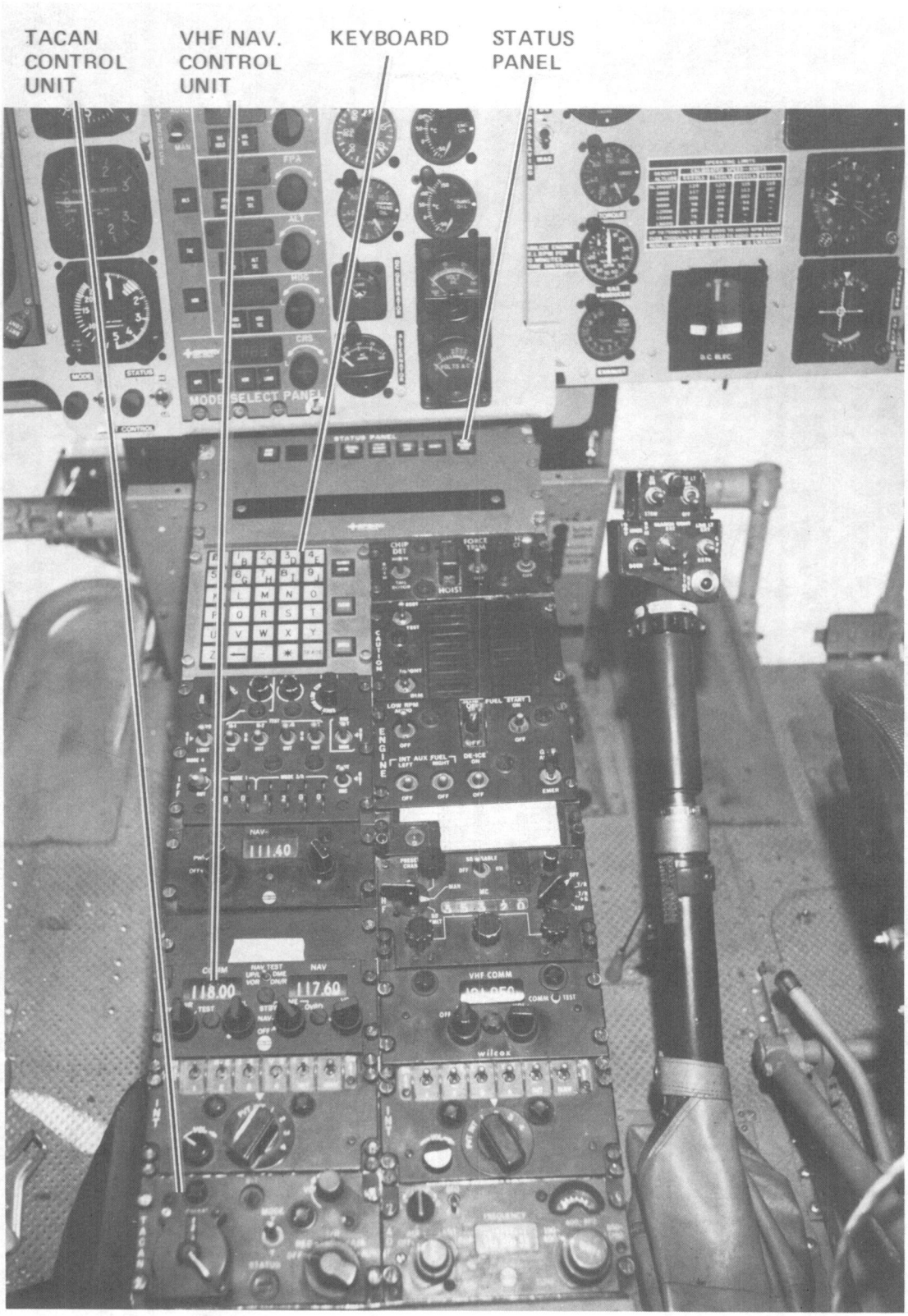

Figure 5.– The center console.

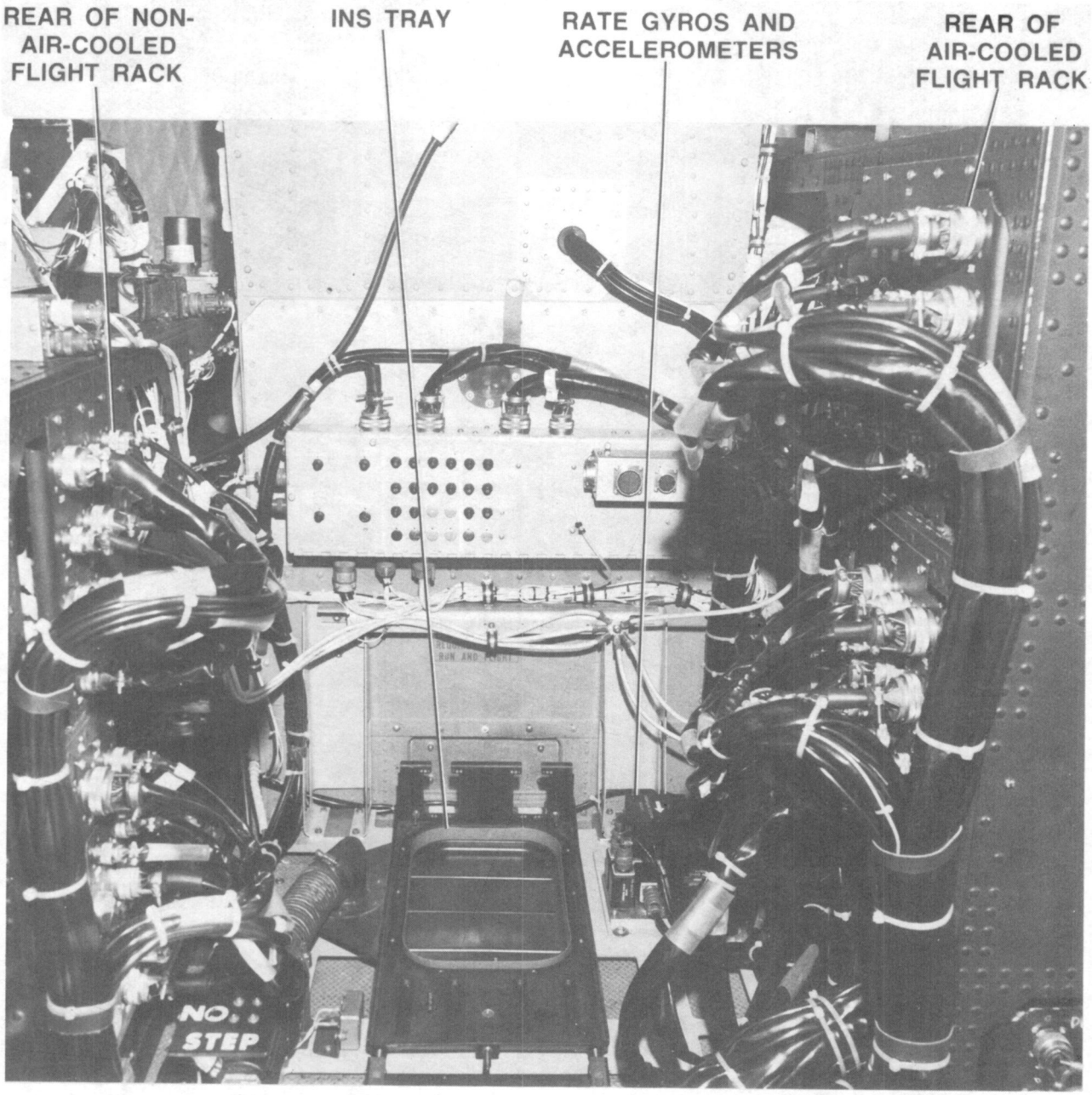

Figure 6.– View toward the rear looking between the flight racks showing the inertial platform.

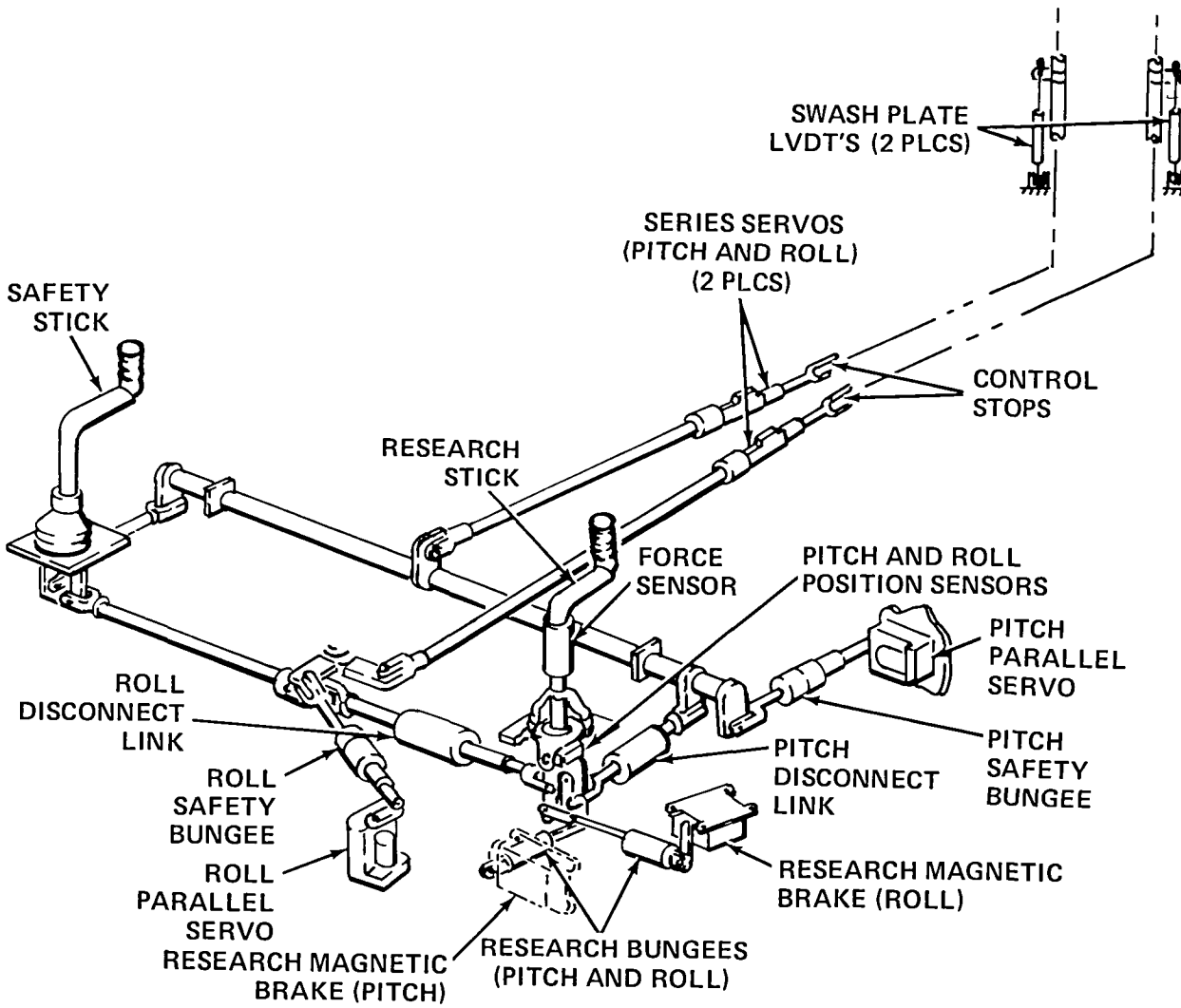

(a) Cyclic controls.

Figure 7.– Control System.

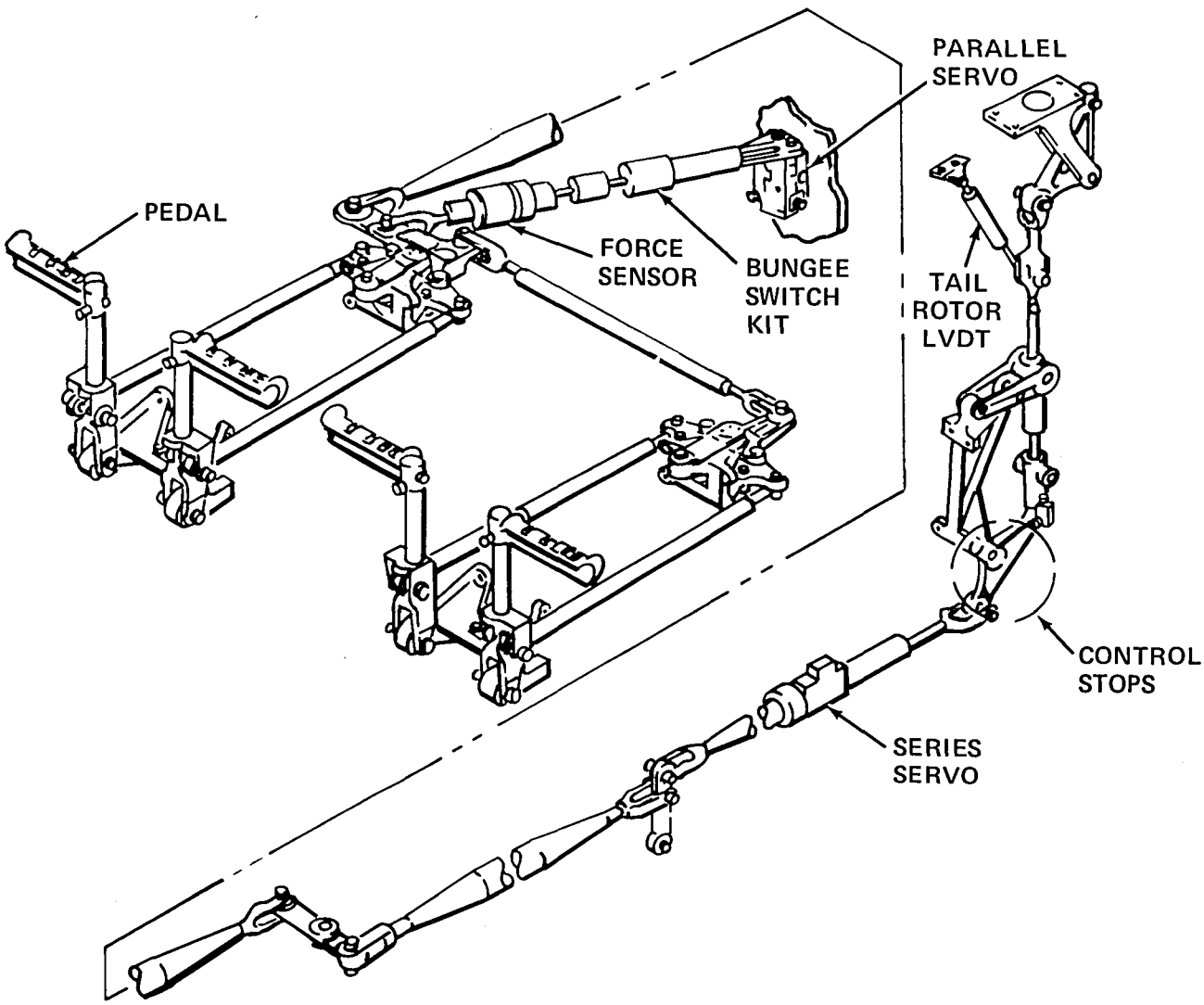

(b) Directional controls.

Figure 7.– Continued.

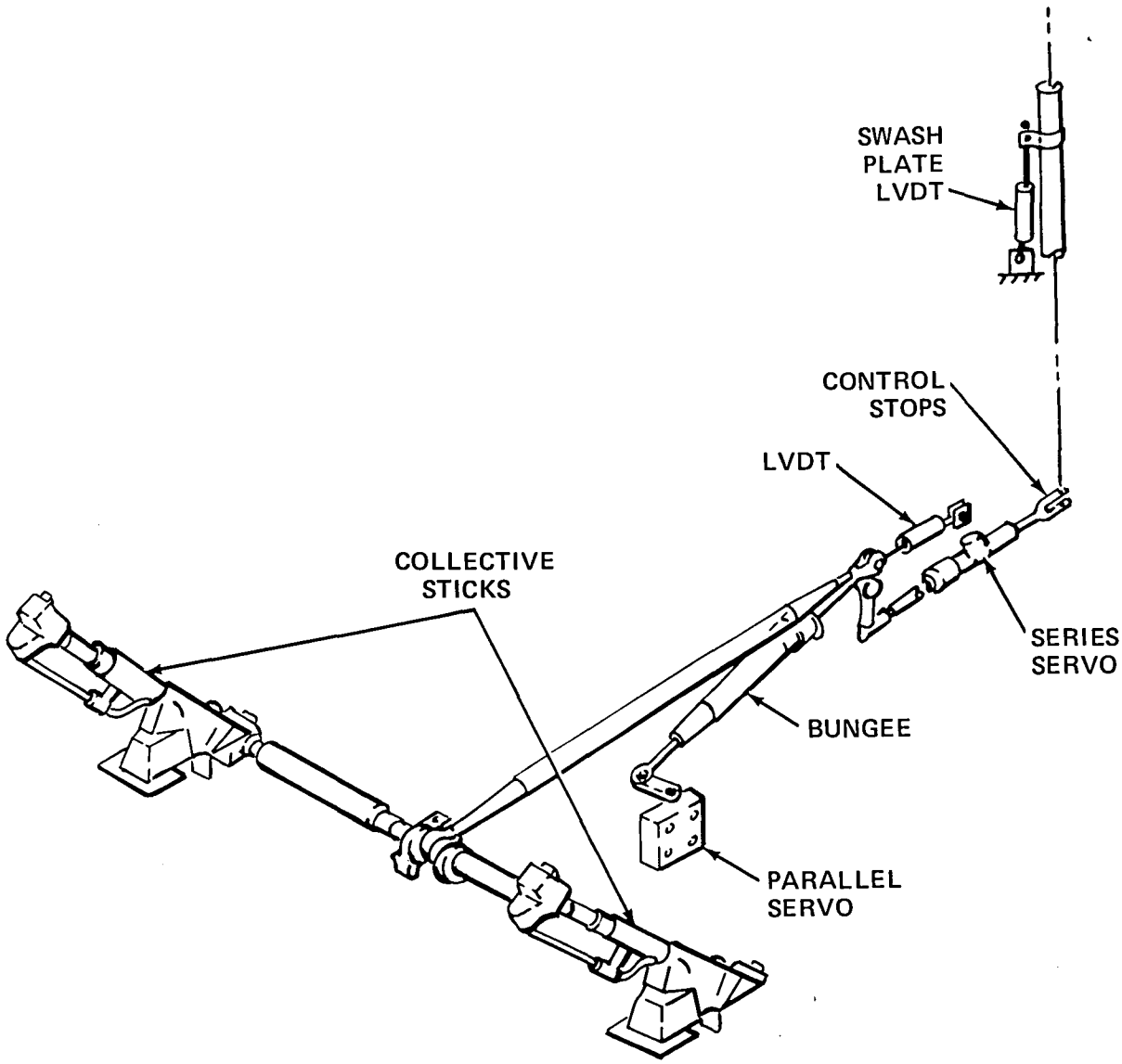

(c) Collective controls.

Figure 7.– Concluded.

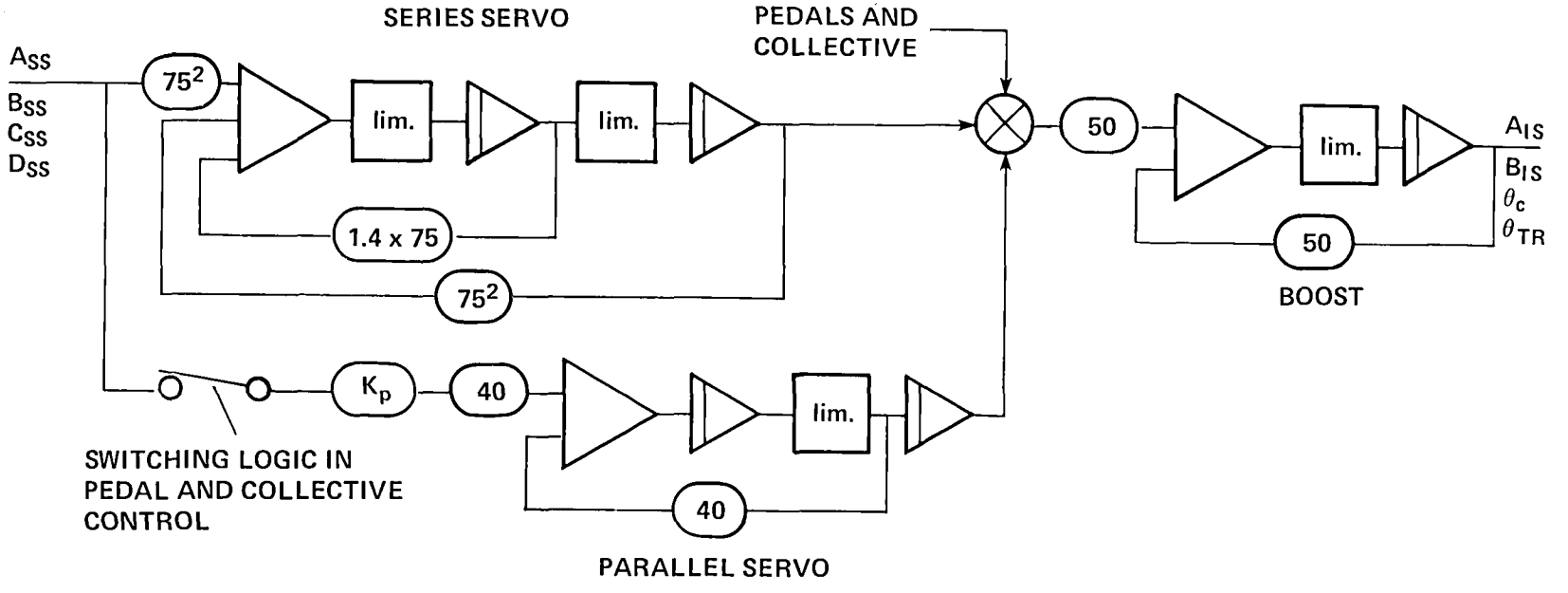

Figure 8.– Flight-control actuator interconnection diagram.

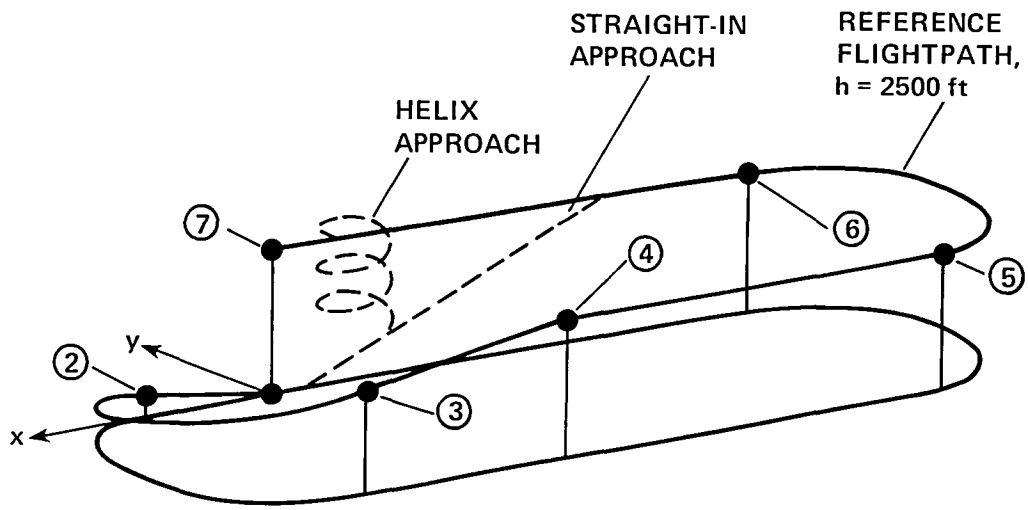

Figure 9.– Reference flightpath and approaches.

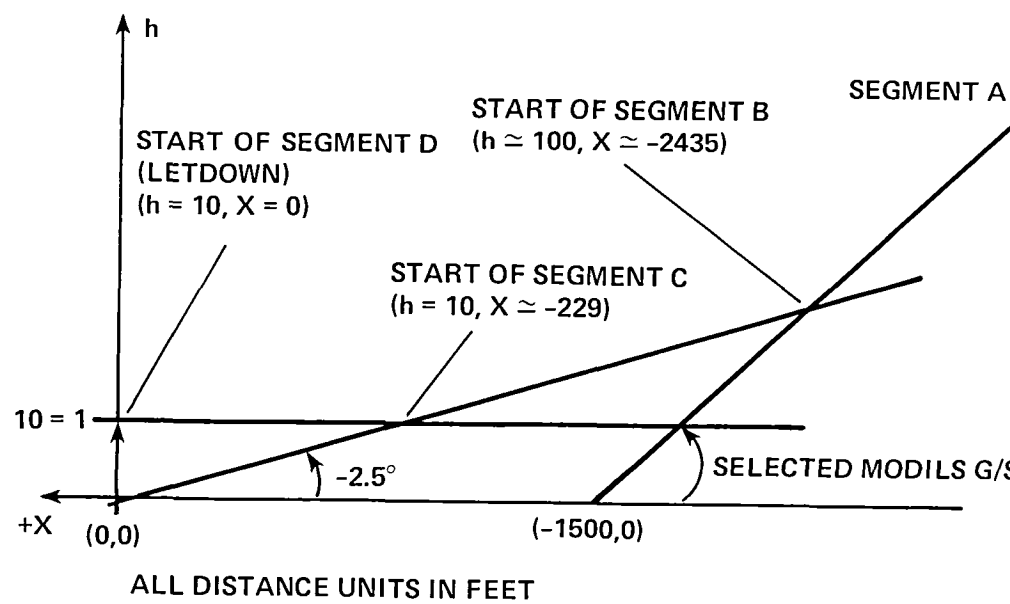

Figure 10.– MODILS straight-in landing approach (elevation view).

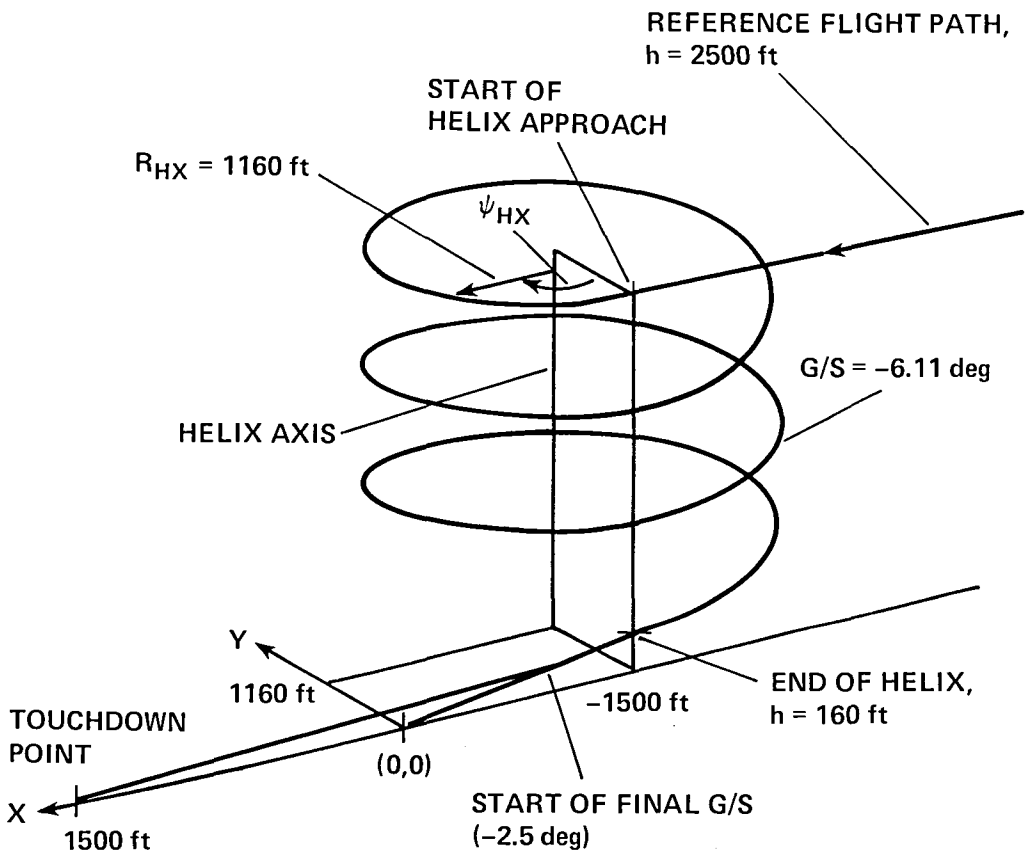

Figure 11.– The helix approach trajectory.

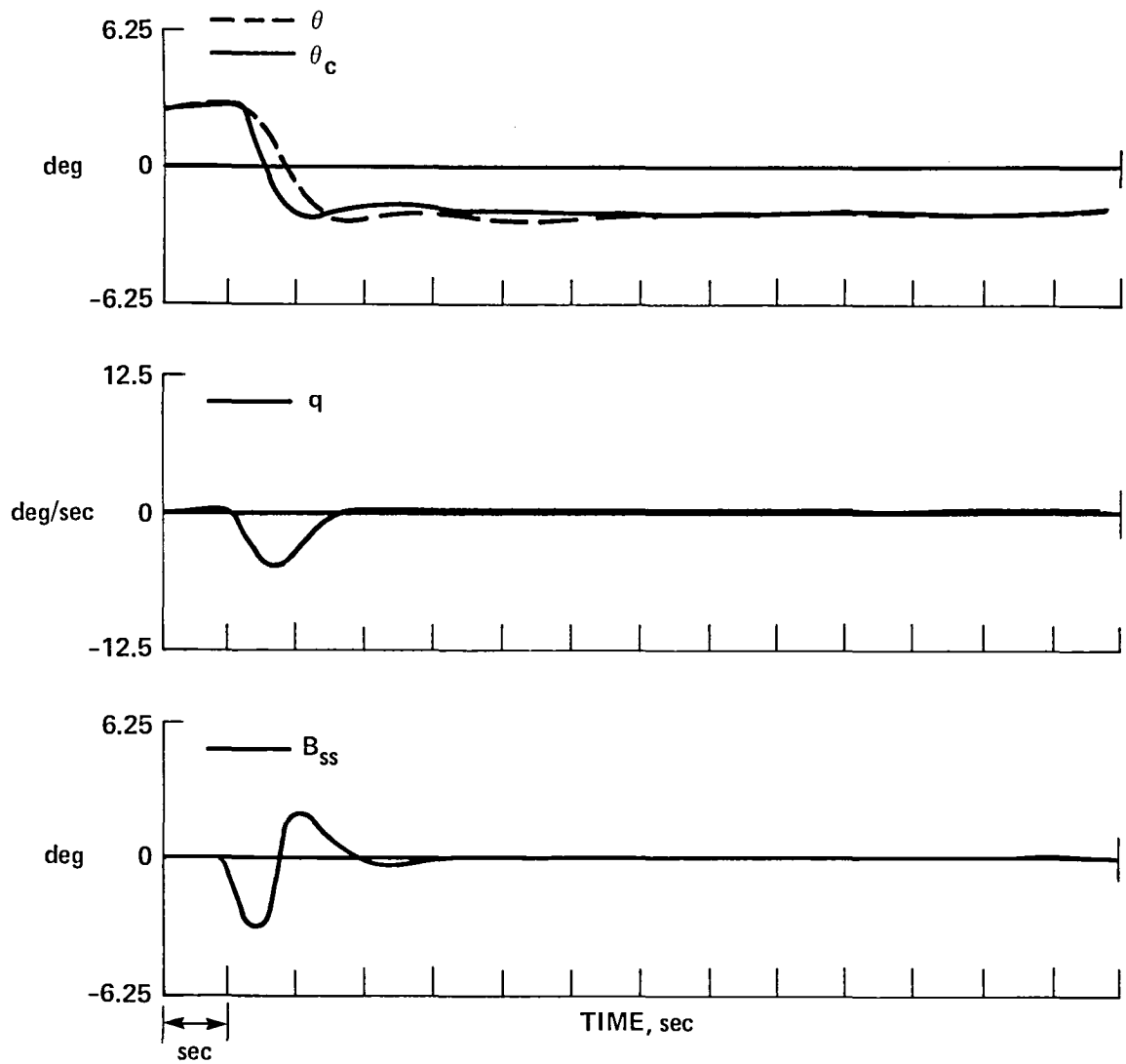

(a) Pitch.

Figure 12.– Simulator step response.

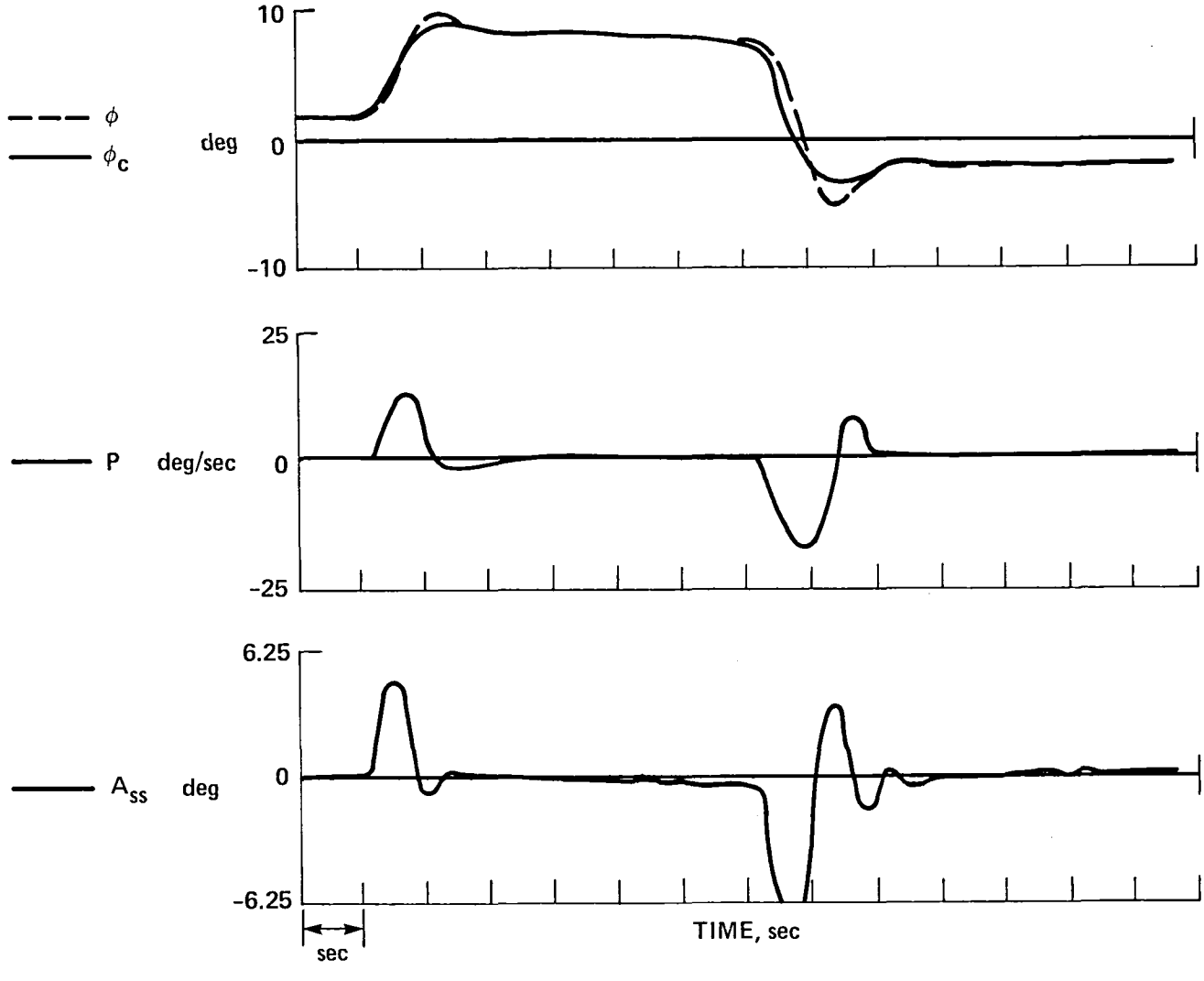

(b) Roll.

Figure 12.– Continued.

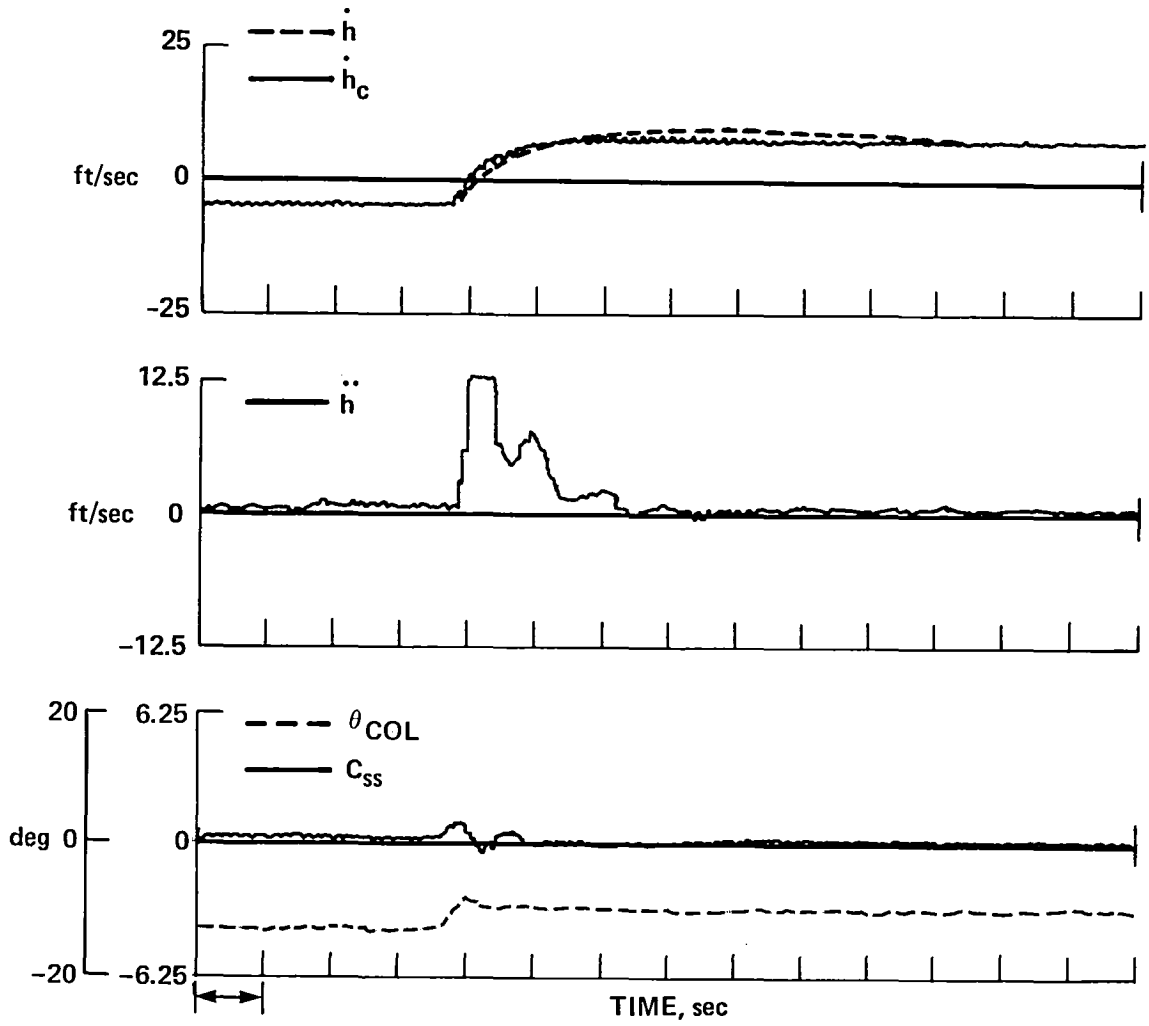

(c) Collective.

Figure 12.– Concluded.

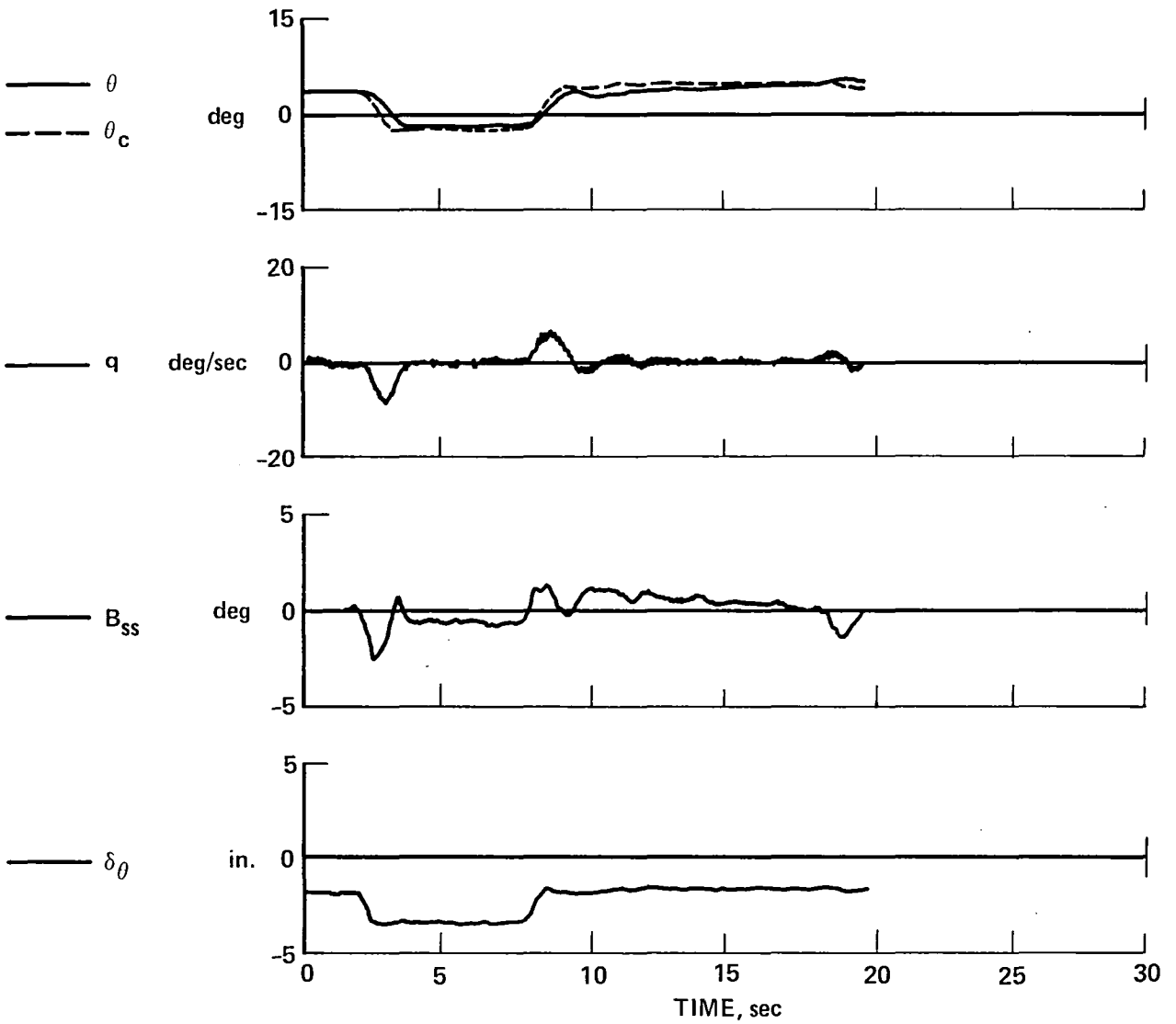

(a) Pitch.

Figure 13.– In-flight step response.

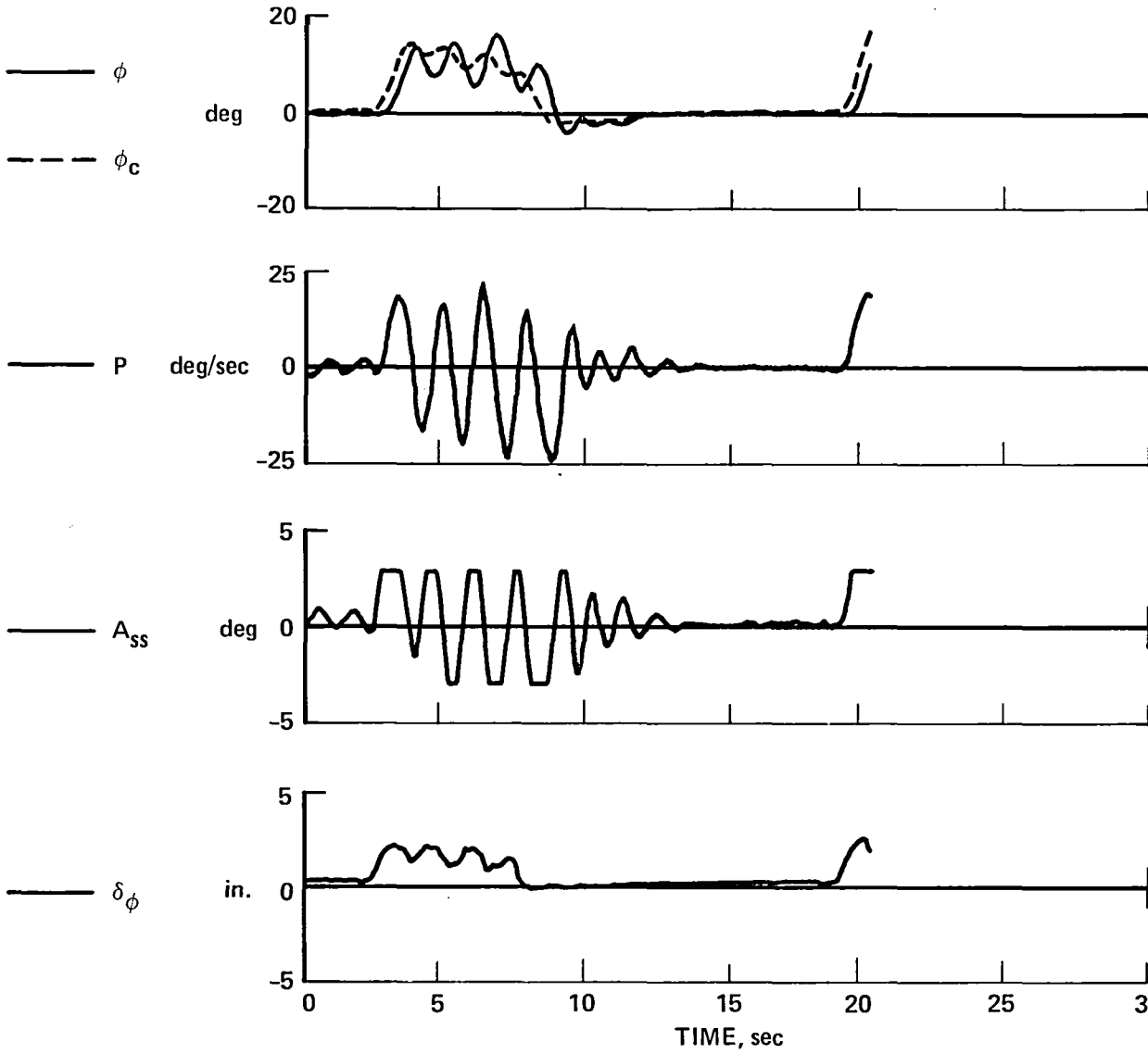

(b) Roll.

Figure 13.– Continued.

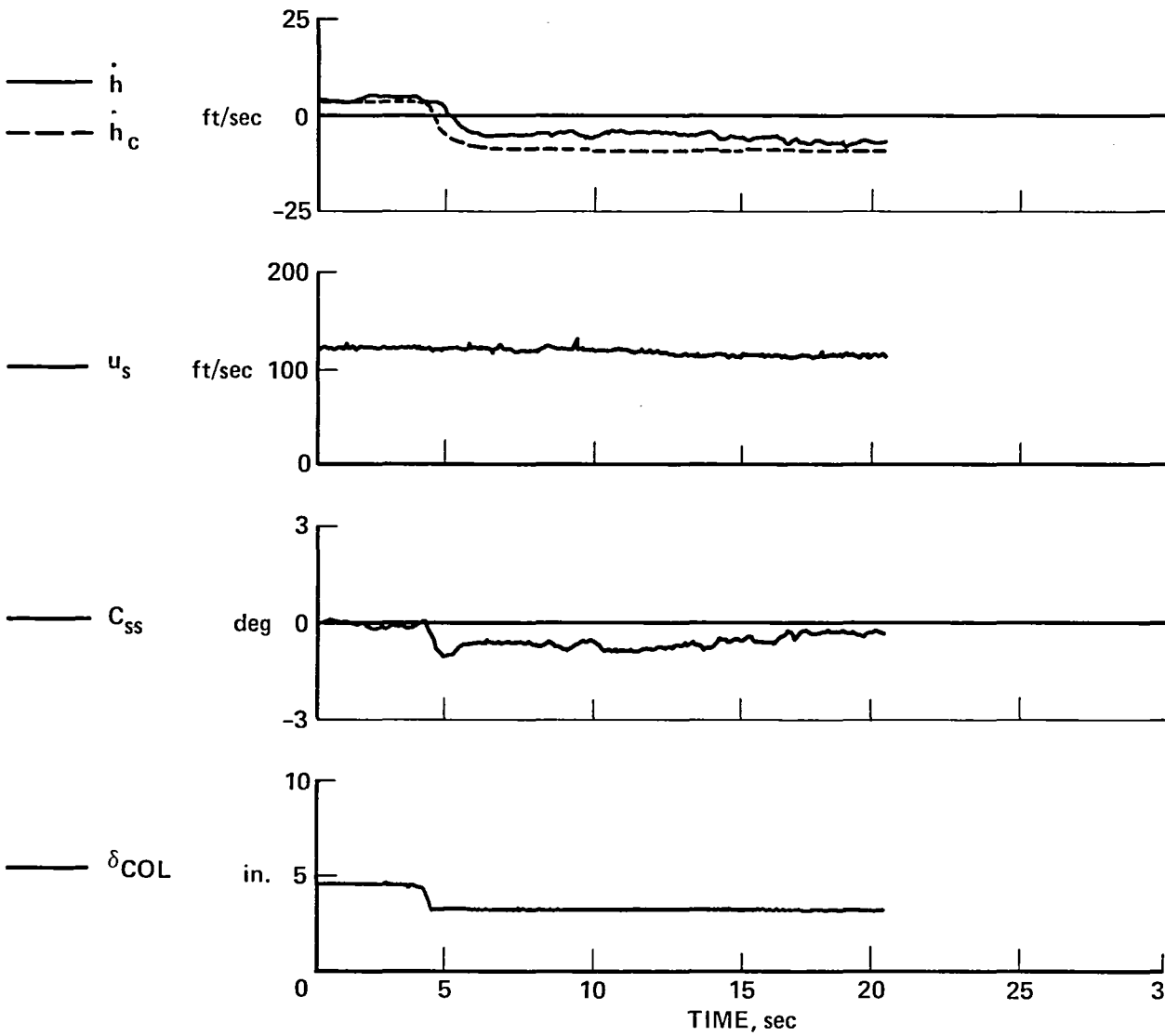

(c) Collective.

Figure 13.– Concluded.

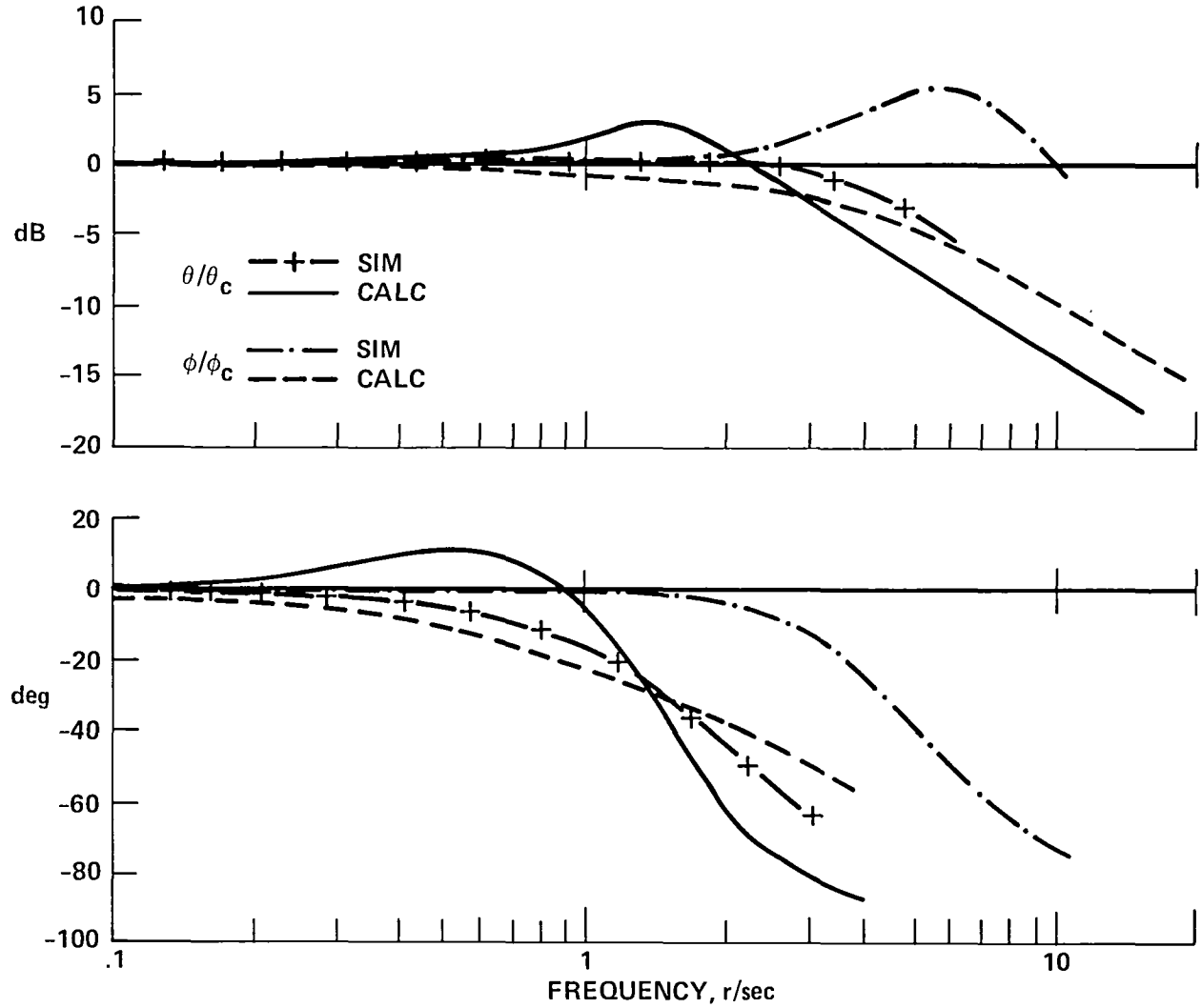

Figure 14.– CSS pitch and roll frequency response.

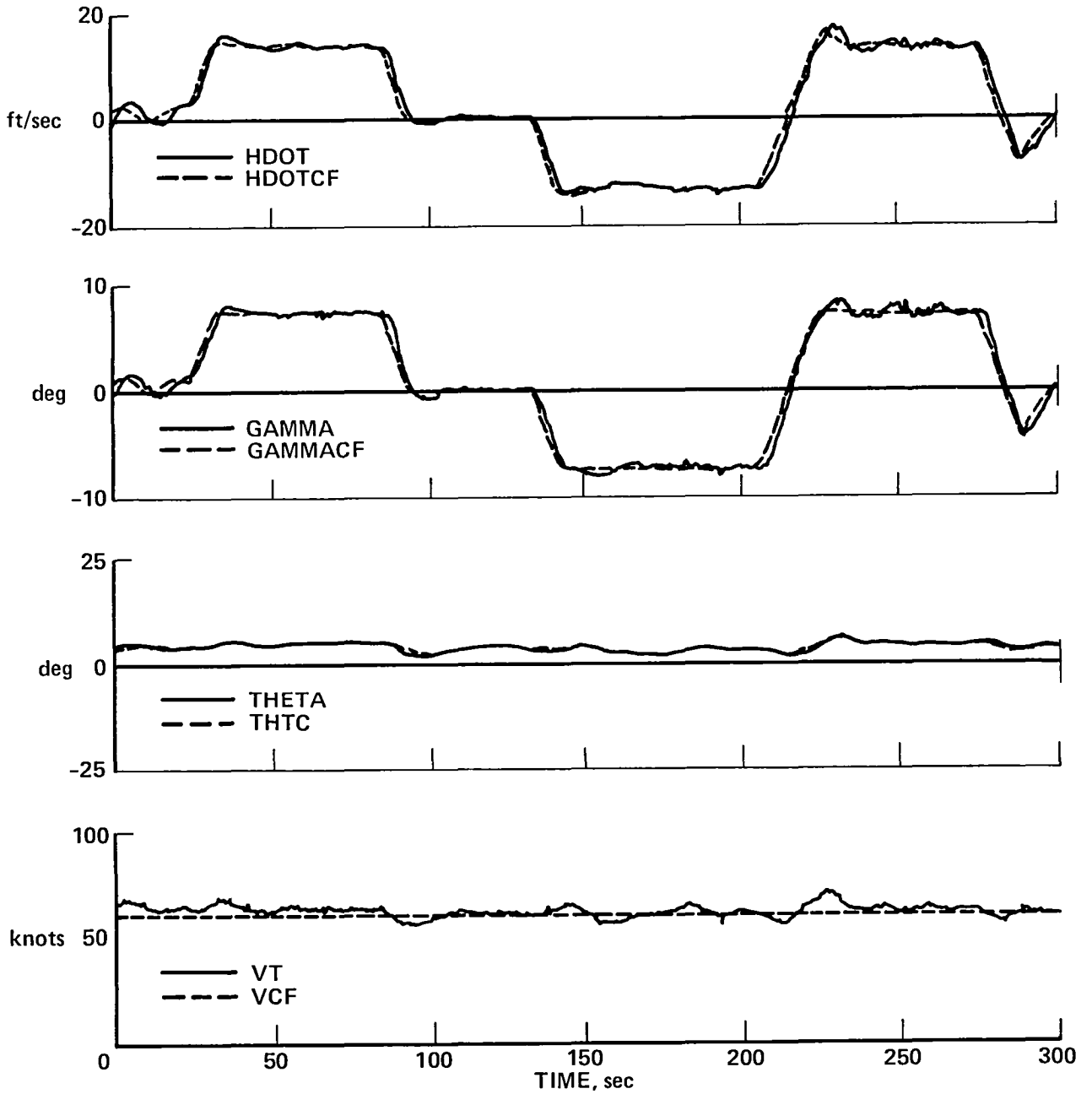

Figure 15.– Flightpath angle SEL/HLD performance.

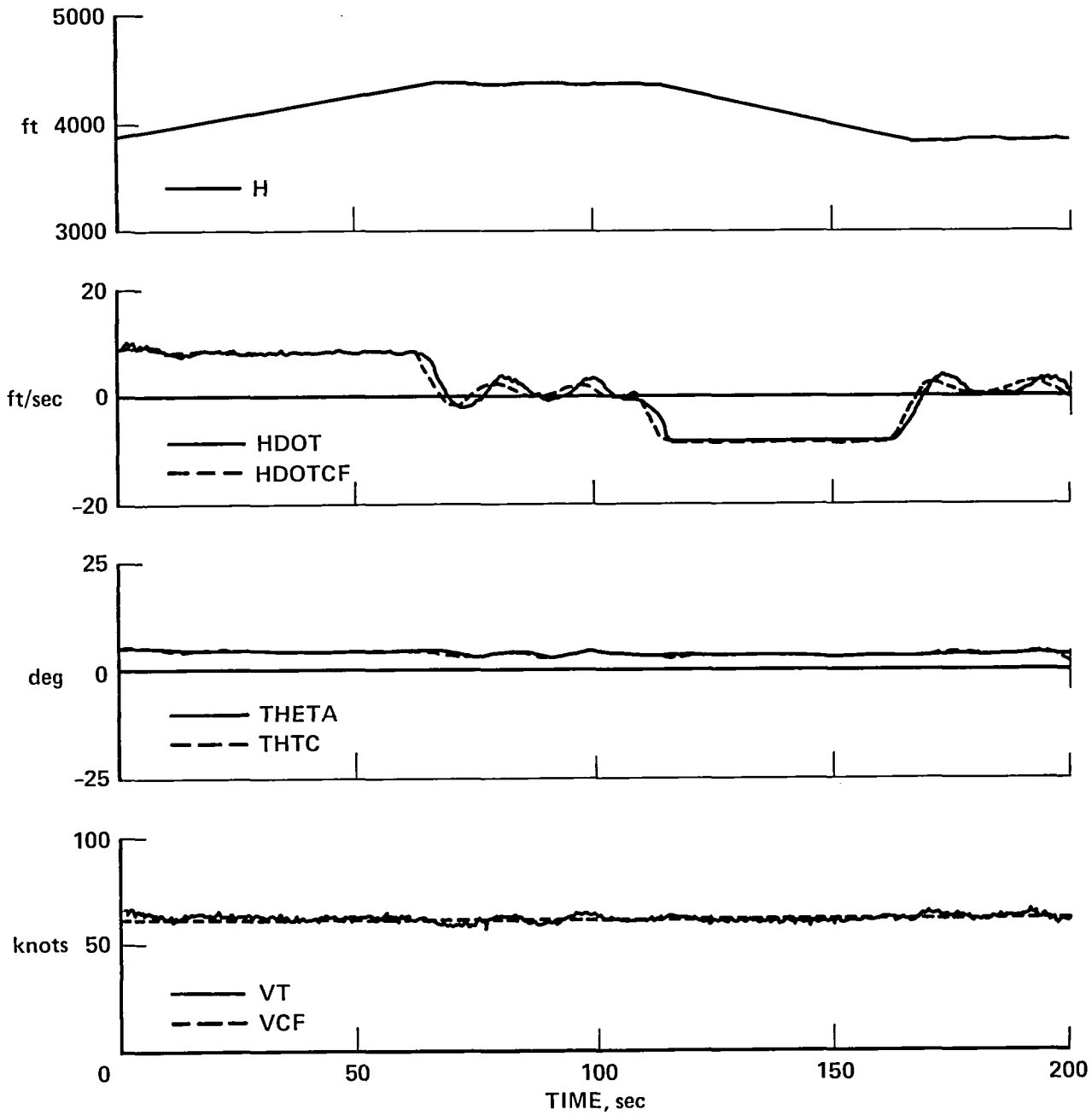

Figure 16.– Altitude select/hold performance.

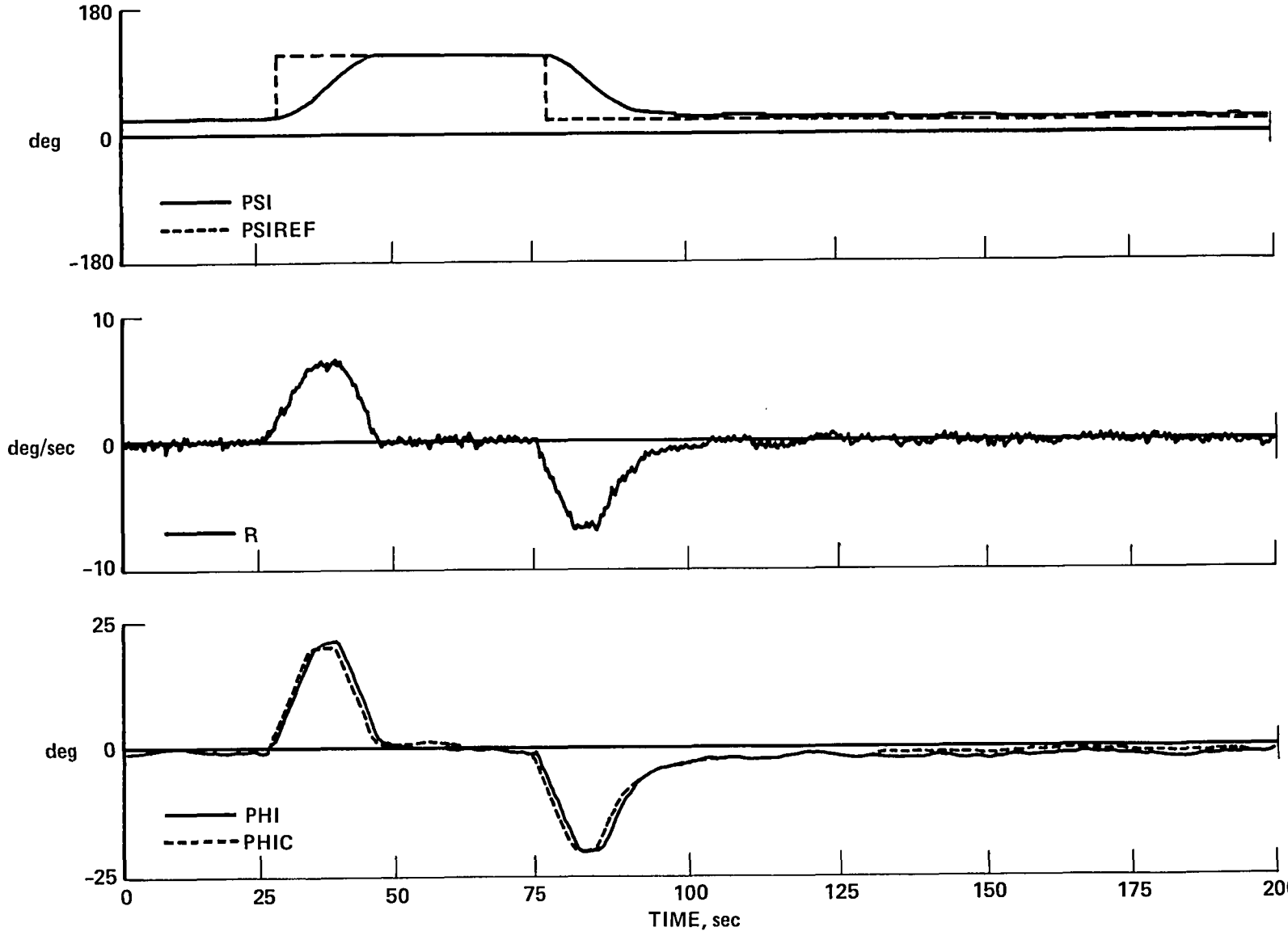

Figure 17.– Heading select/hold performance.

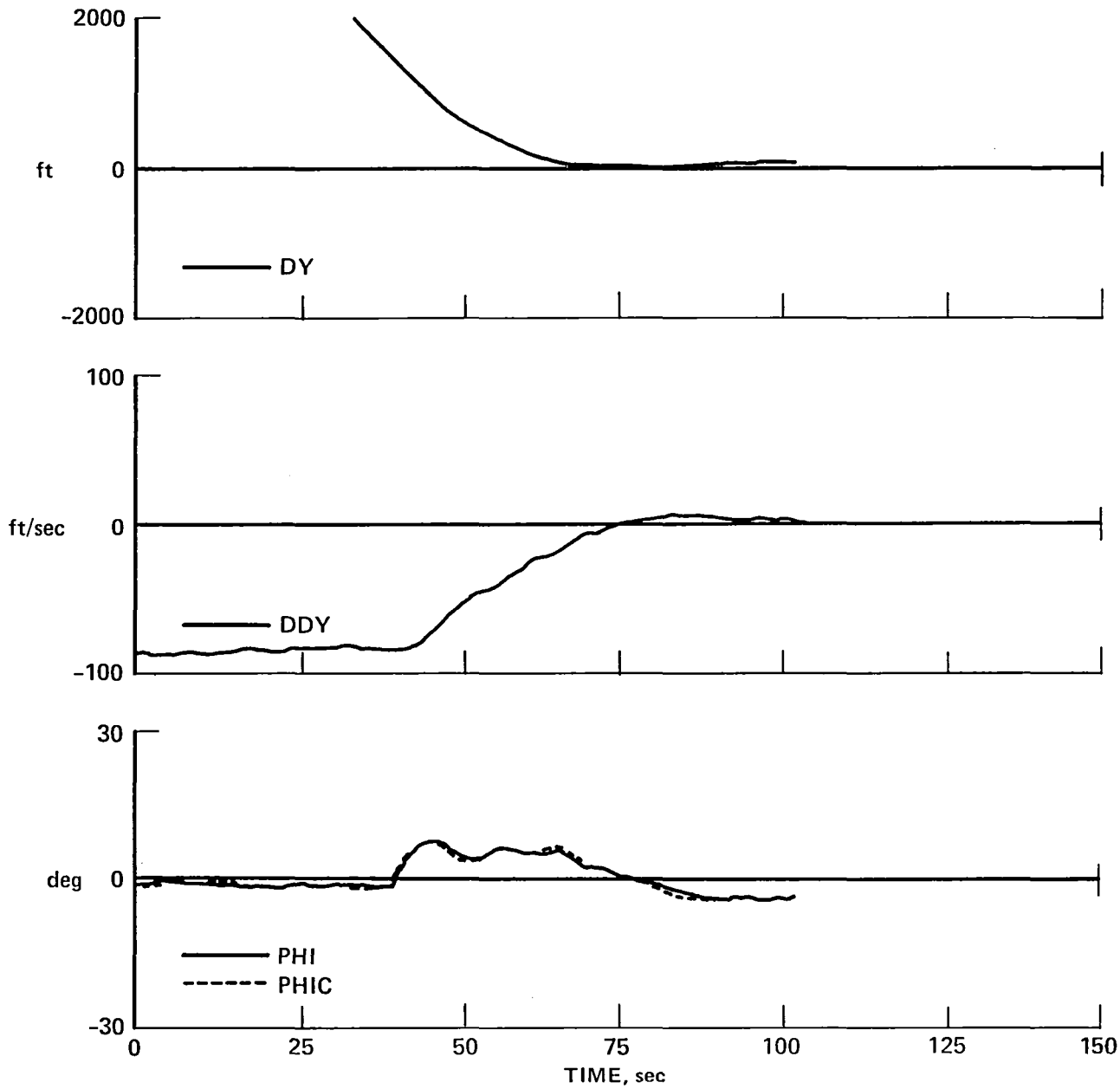

Figure 18.– TACAN capture performance.

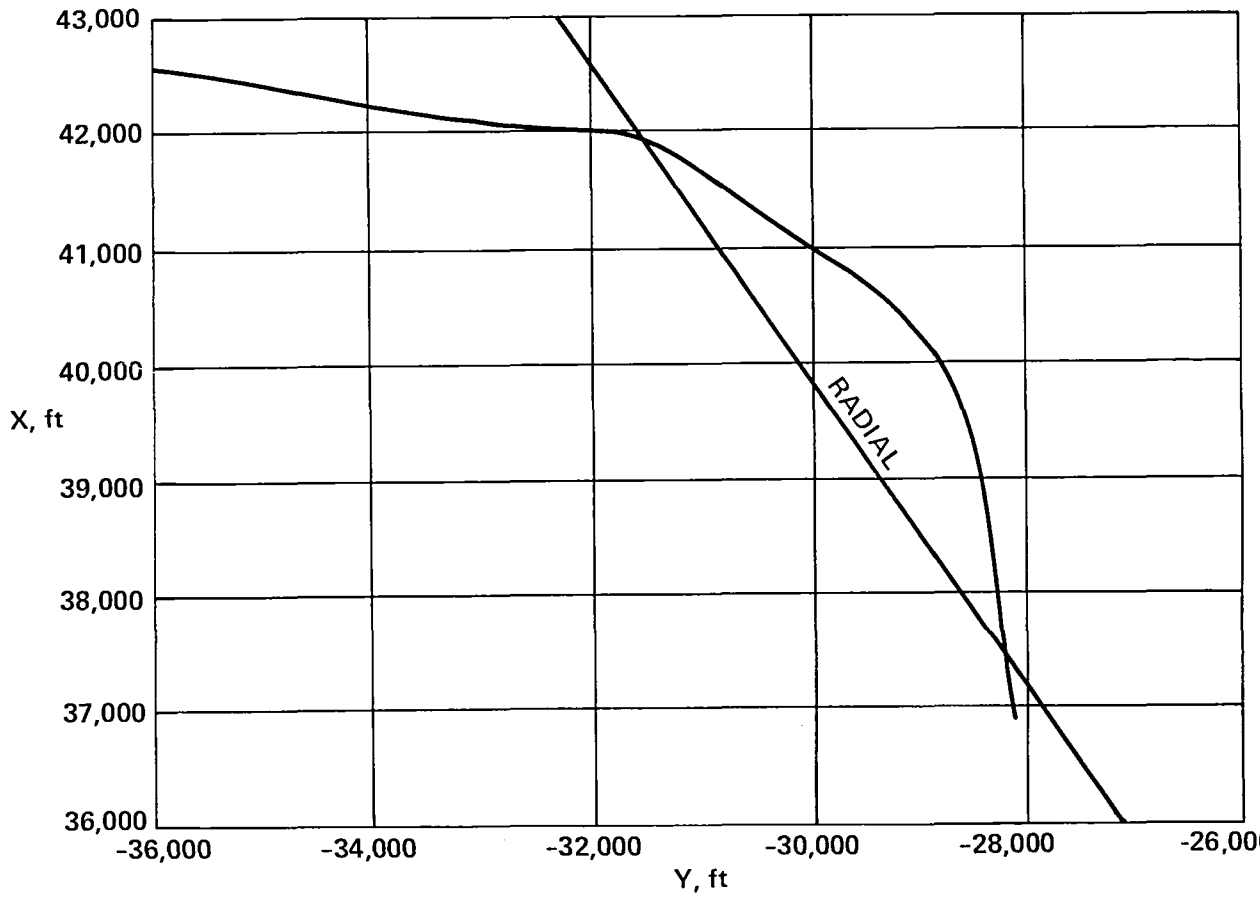

Figure 19.– X–Y plot of TACAN capture (navigation).

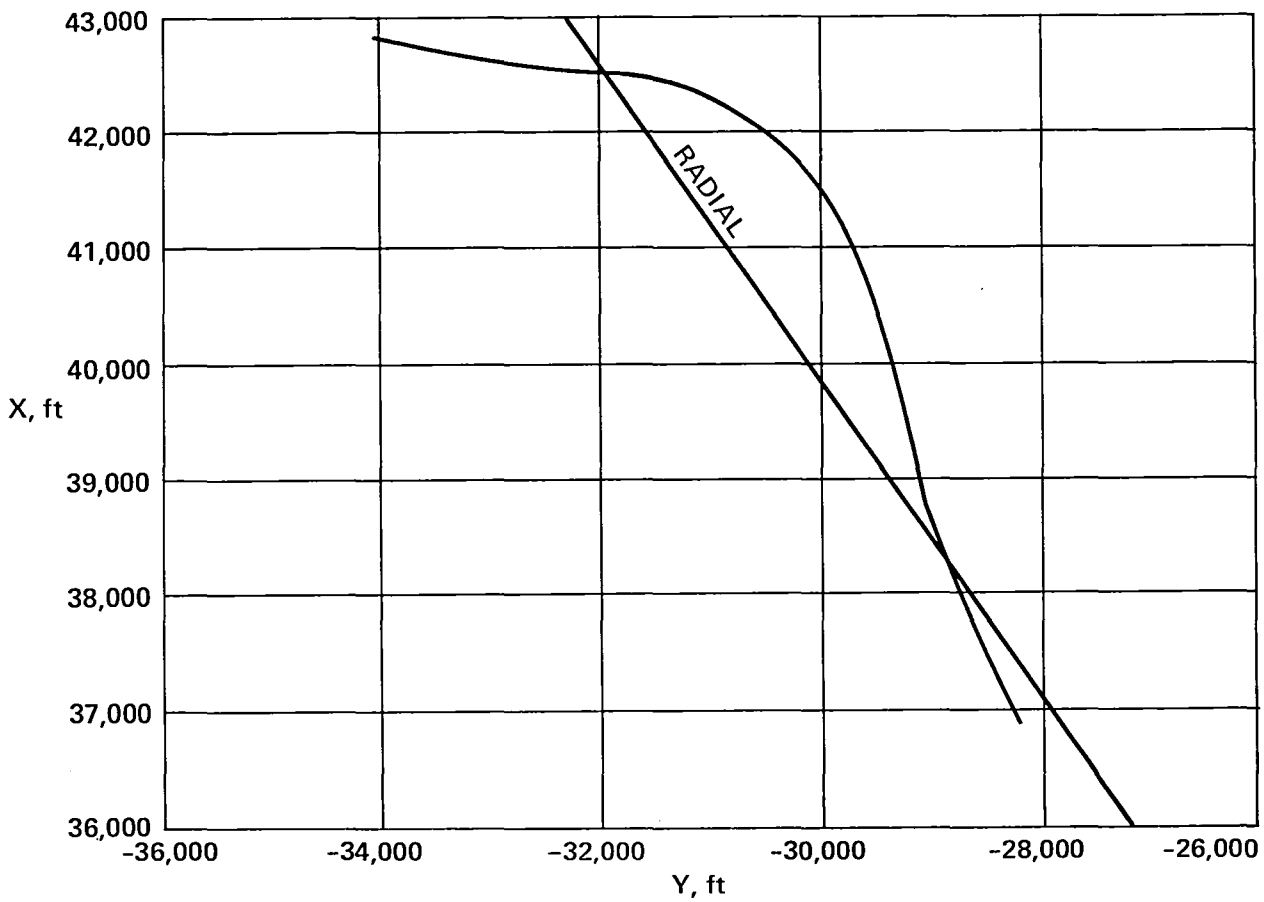

Figure 20.– X–Y plot of TACAN capture (radar).

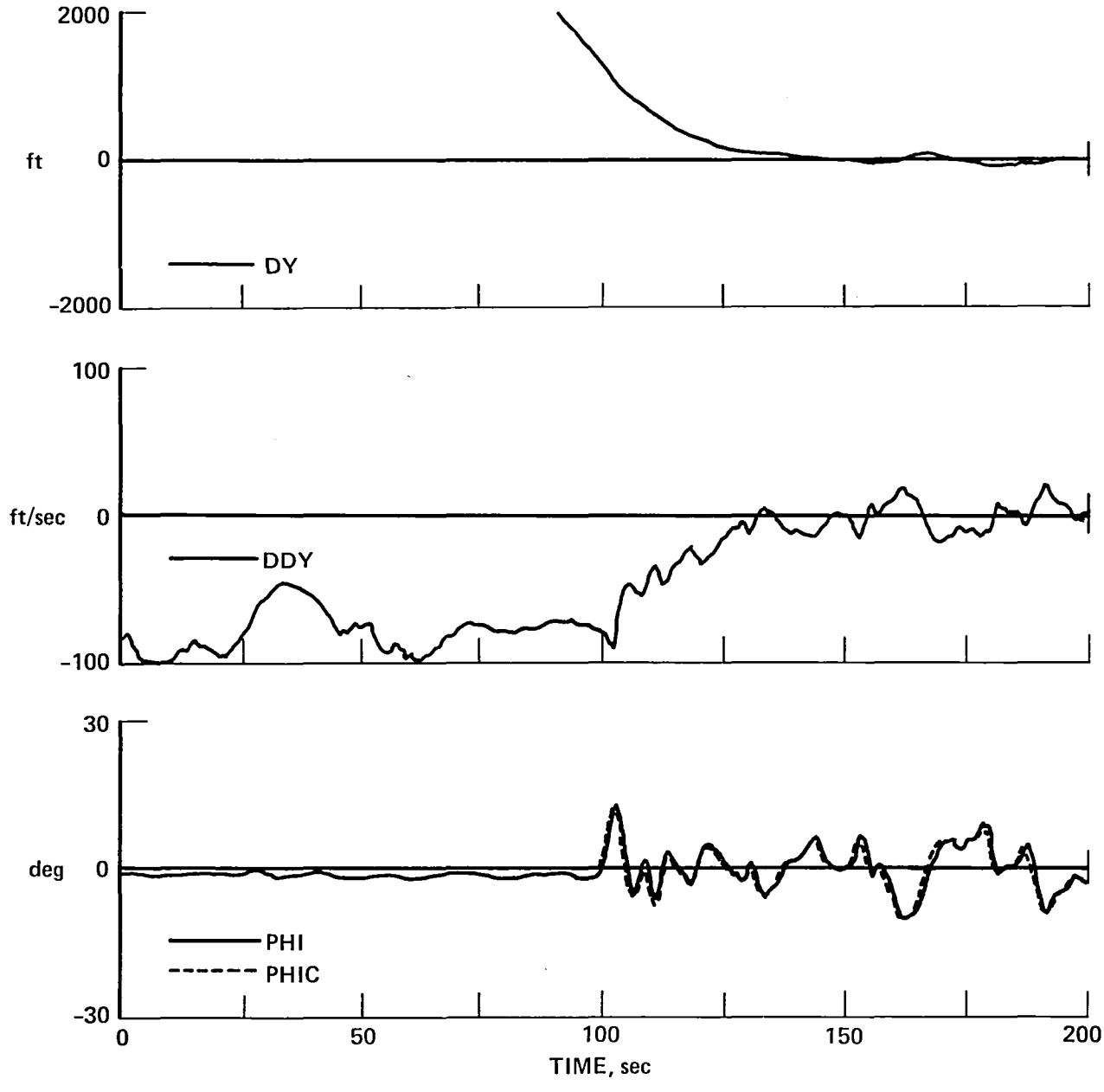

Figure 21.– VOR capture performance.

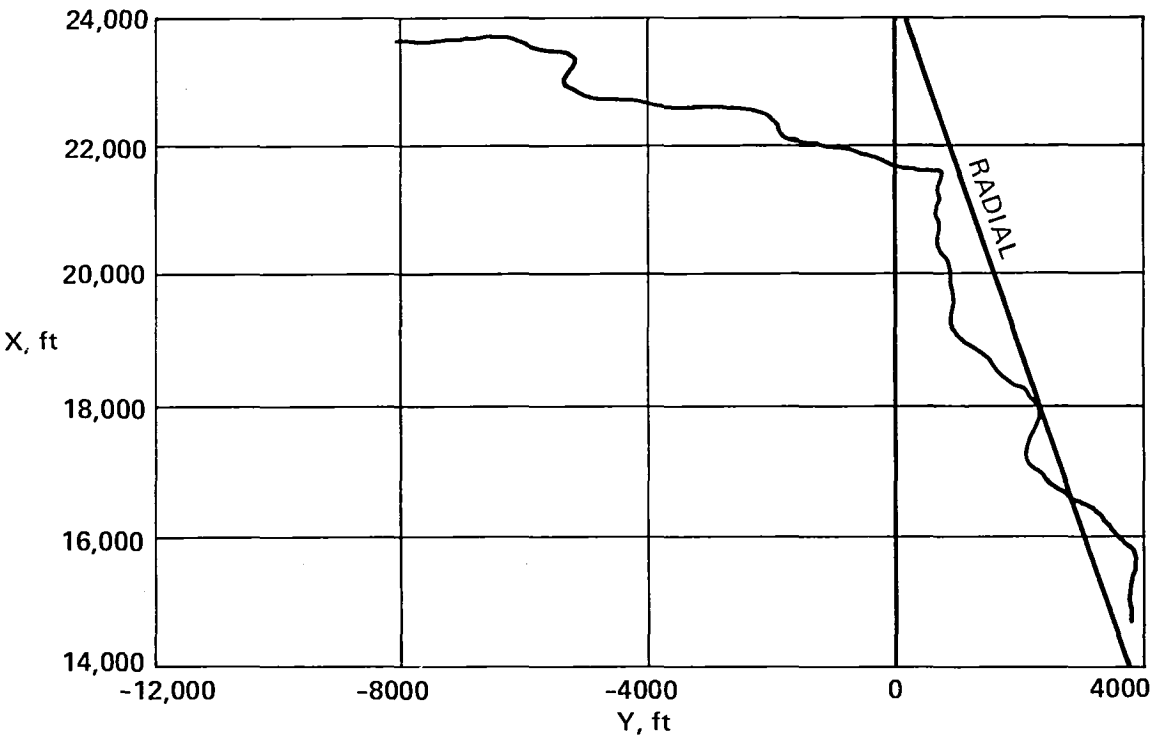

Figure 22.– X–Y plot of VOR capture (navigation).

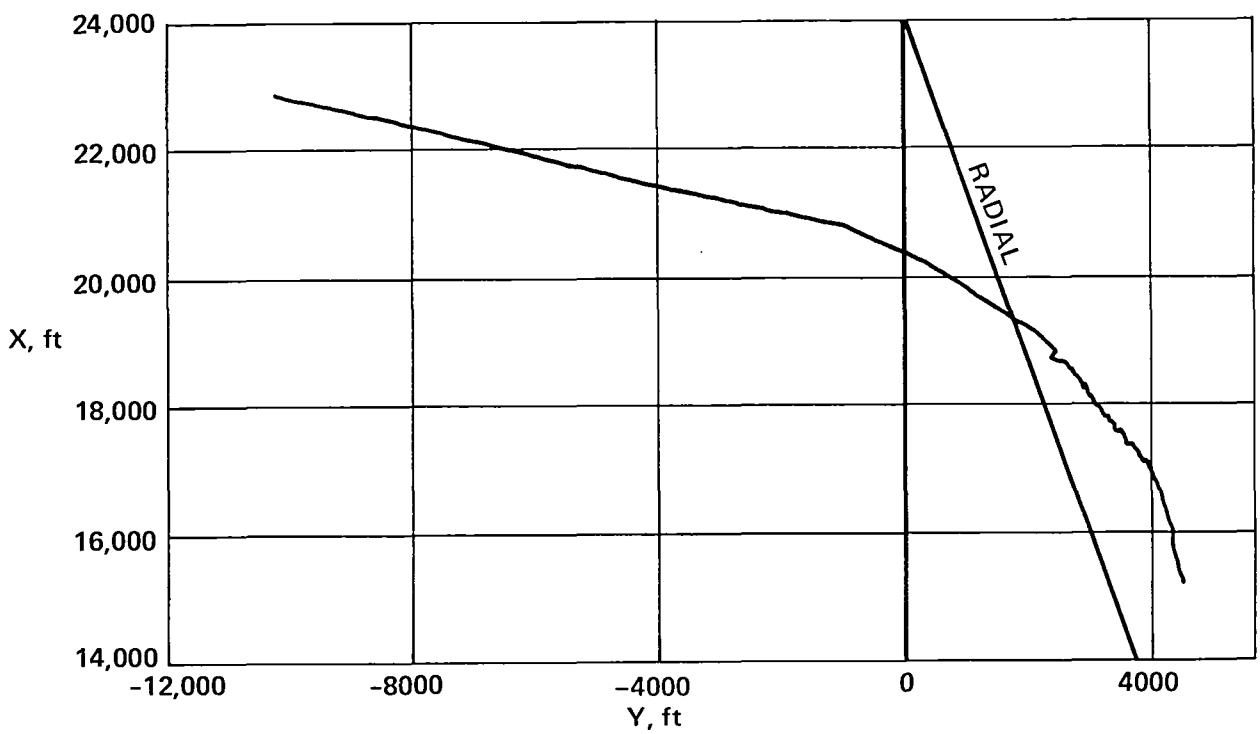

Figure 23.– X–Y plot of VOR capture (radar).

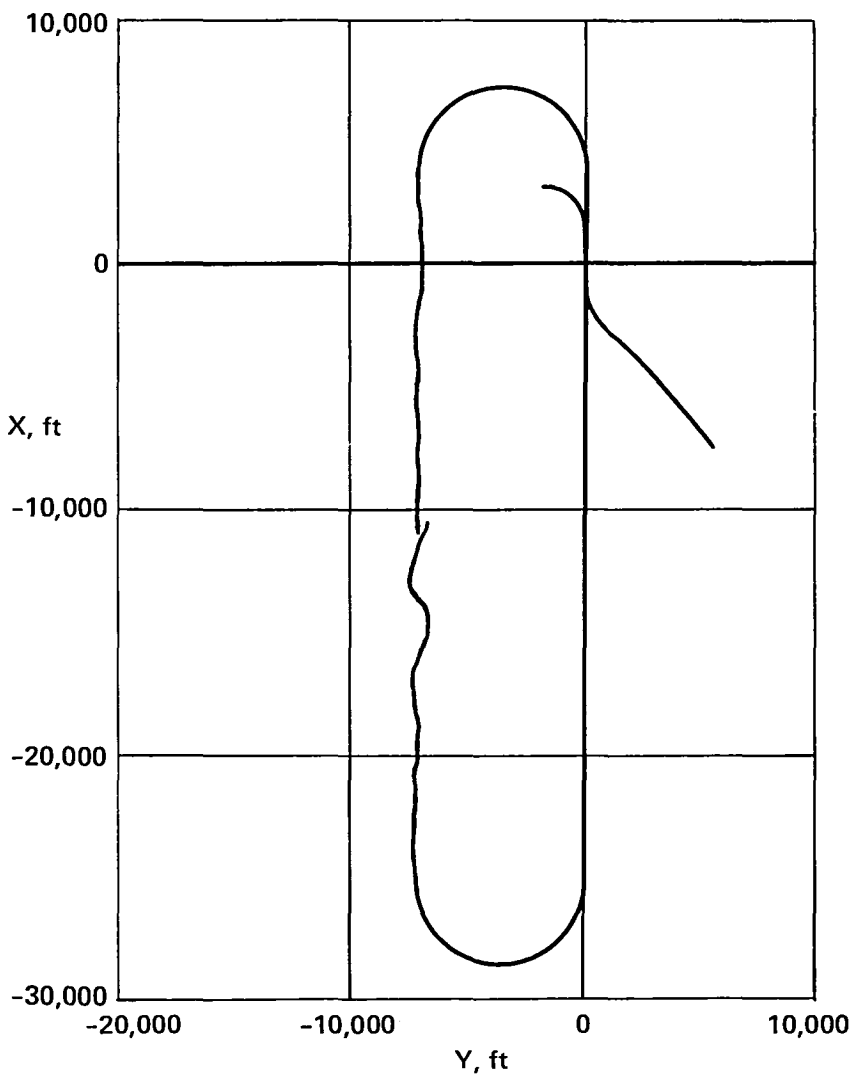

Figure 24.– X–Y plot of reference flightpath.

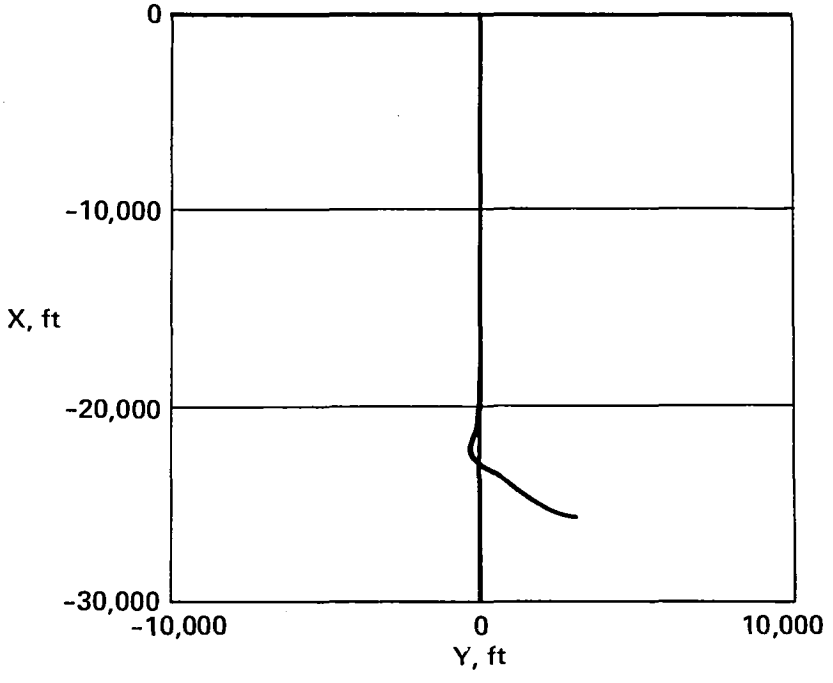

Figure 25.– X–Y plot of straight-in landing, 7.5° glide slope.

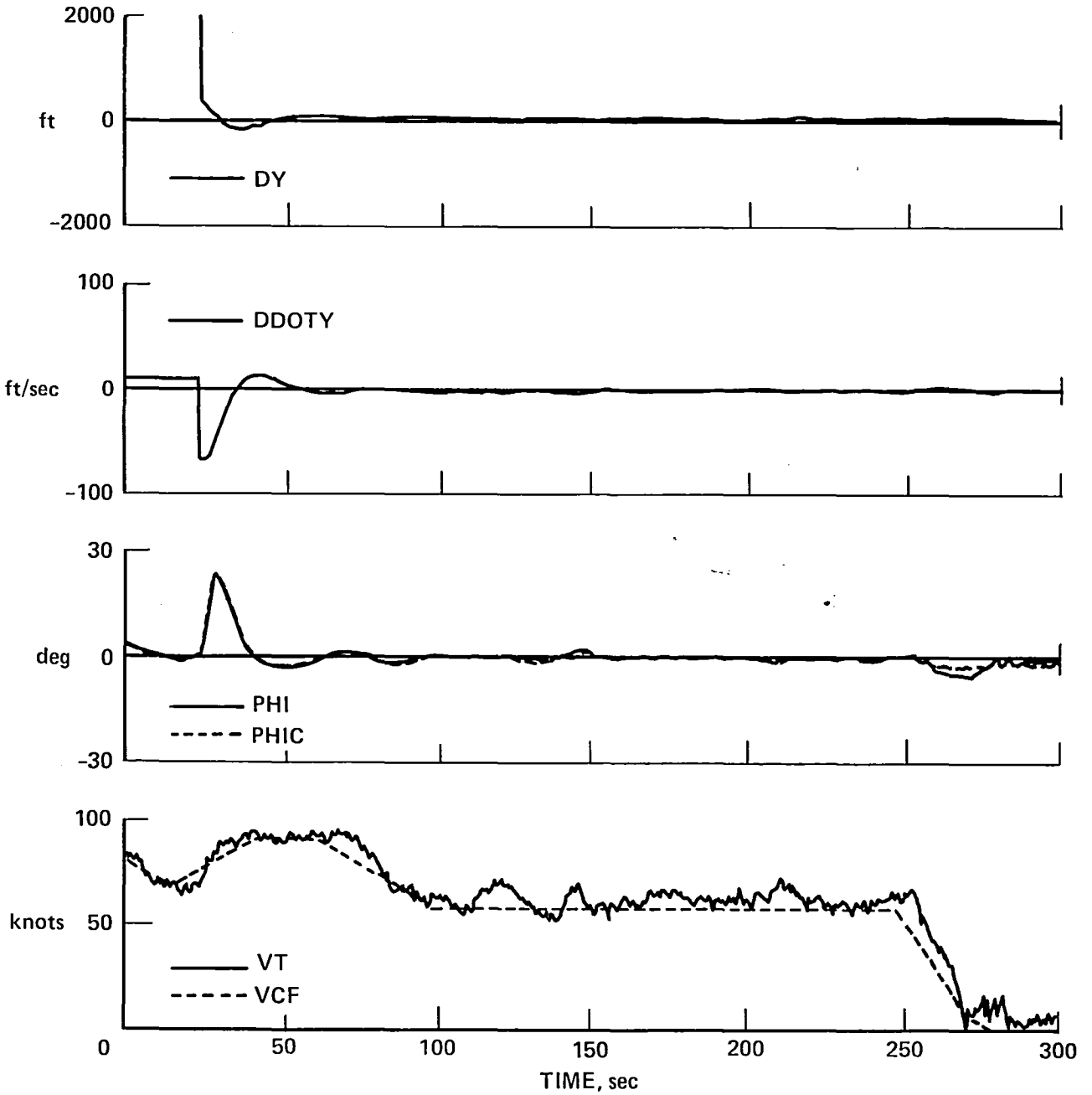

Figure 26.– Straight-in landing performance, 7.5° glide slope.

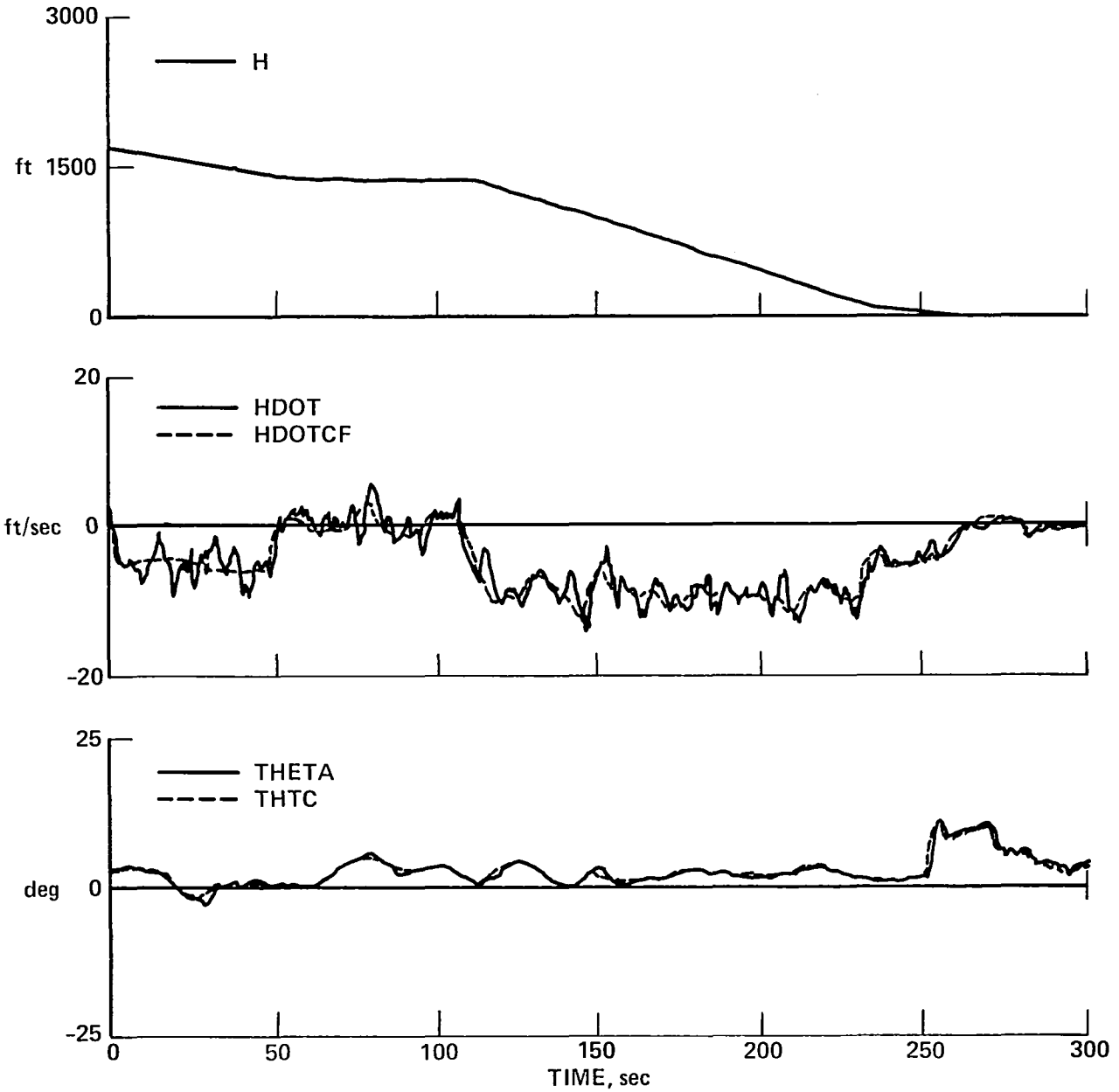

Figure 27.– Straight-in landing performance, 7.5° glide slope.

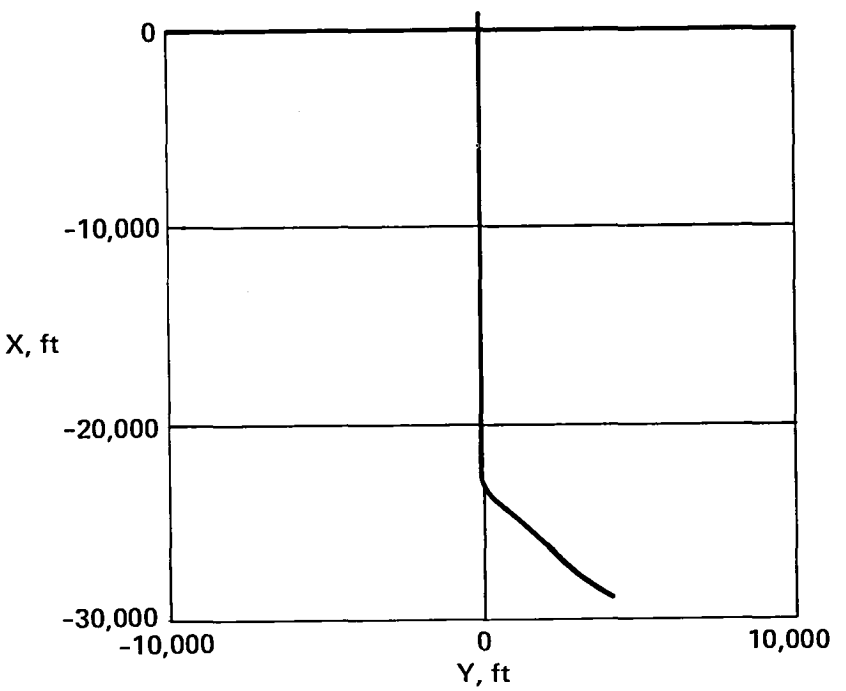

Figure 28.– X–Y plot of straight-in landing, 10° glide slope.

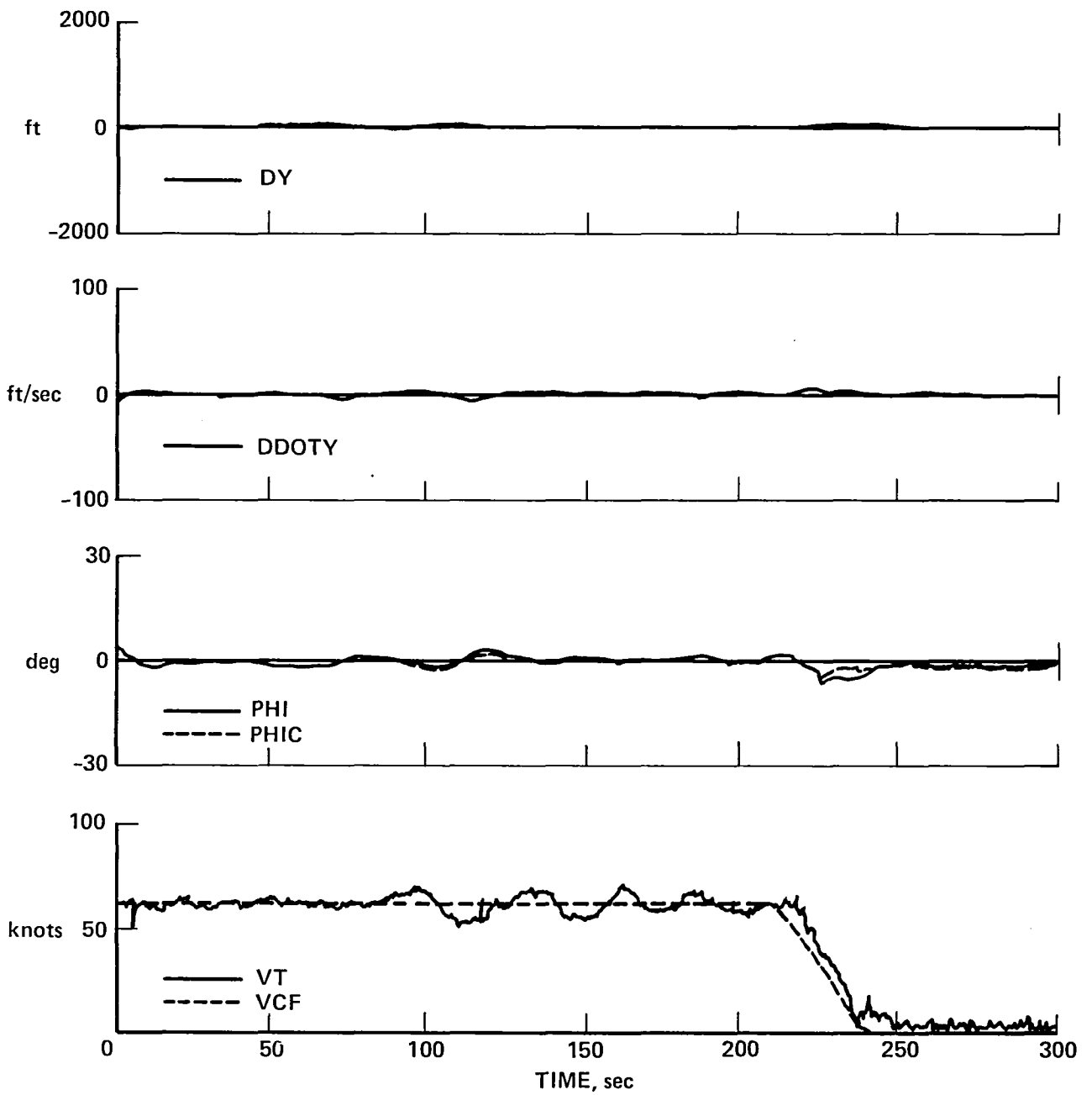

Figure 29.– Straight-in landing performance, 10° glide slope.

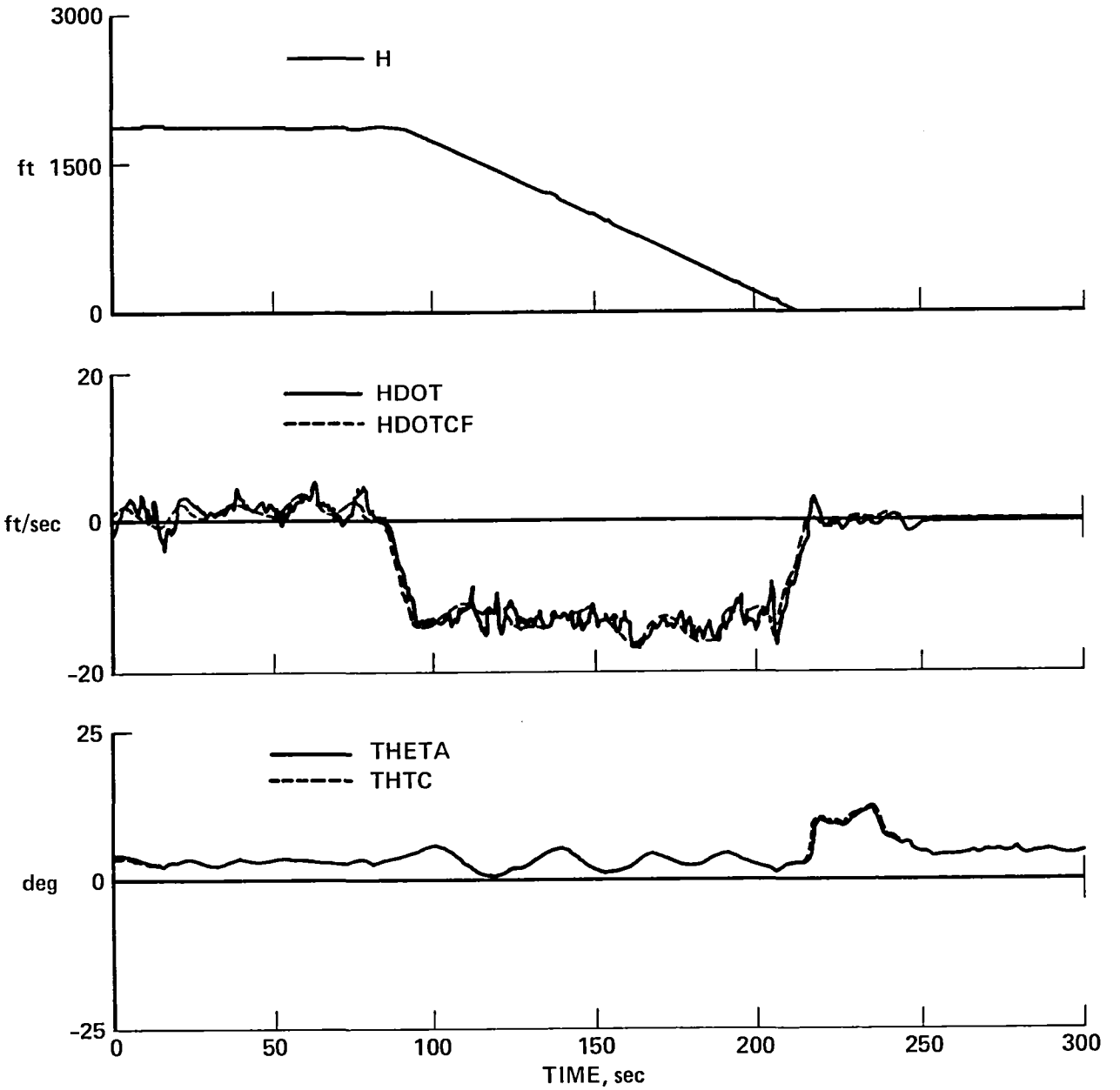

Figure 30.– Straight-in landing performance, 10° glide slope.

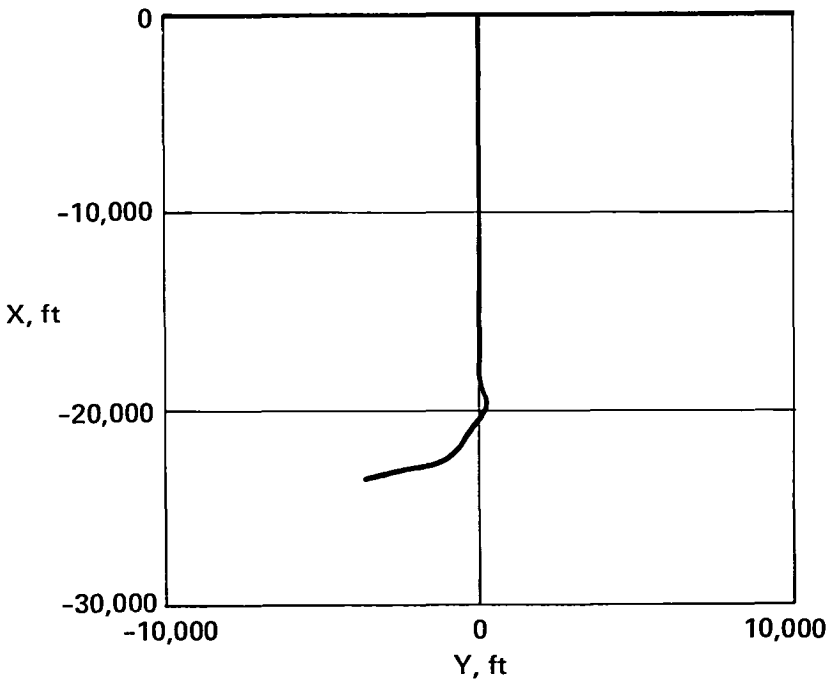

Figure 31.– X–Y plot of straight-in landing, 12.5° glide slope.

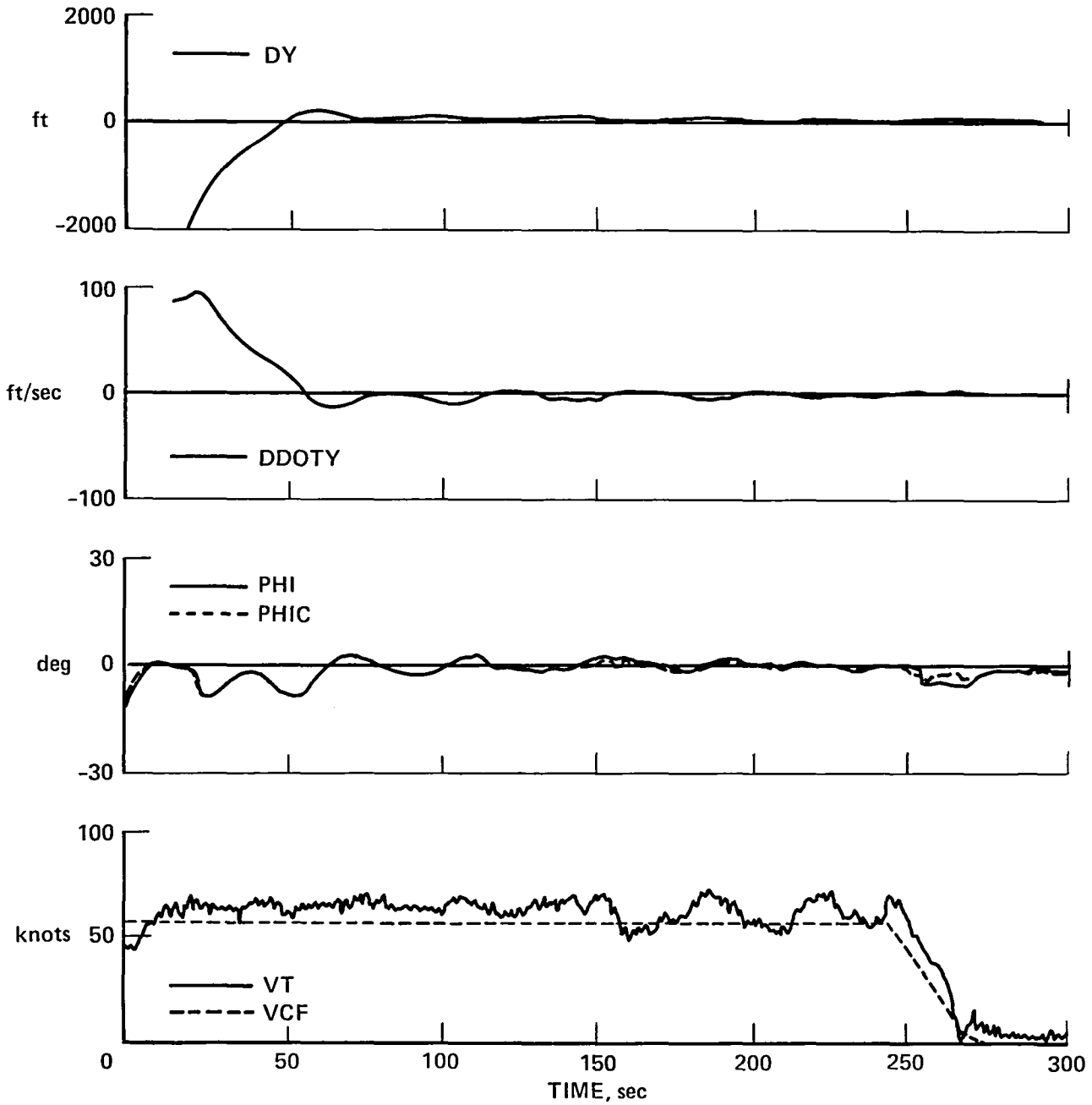

Figure 32.– Straight-in landing performance, 12.5° glide slope.

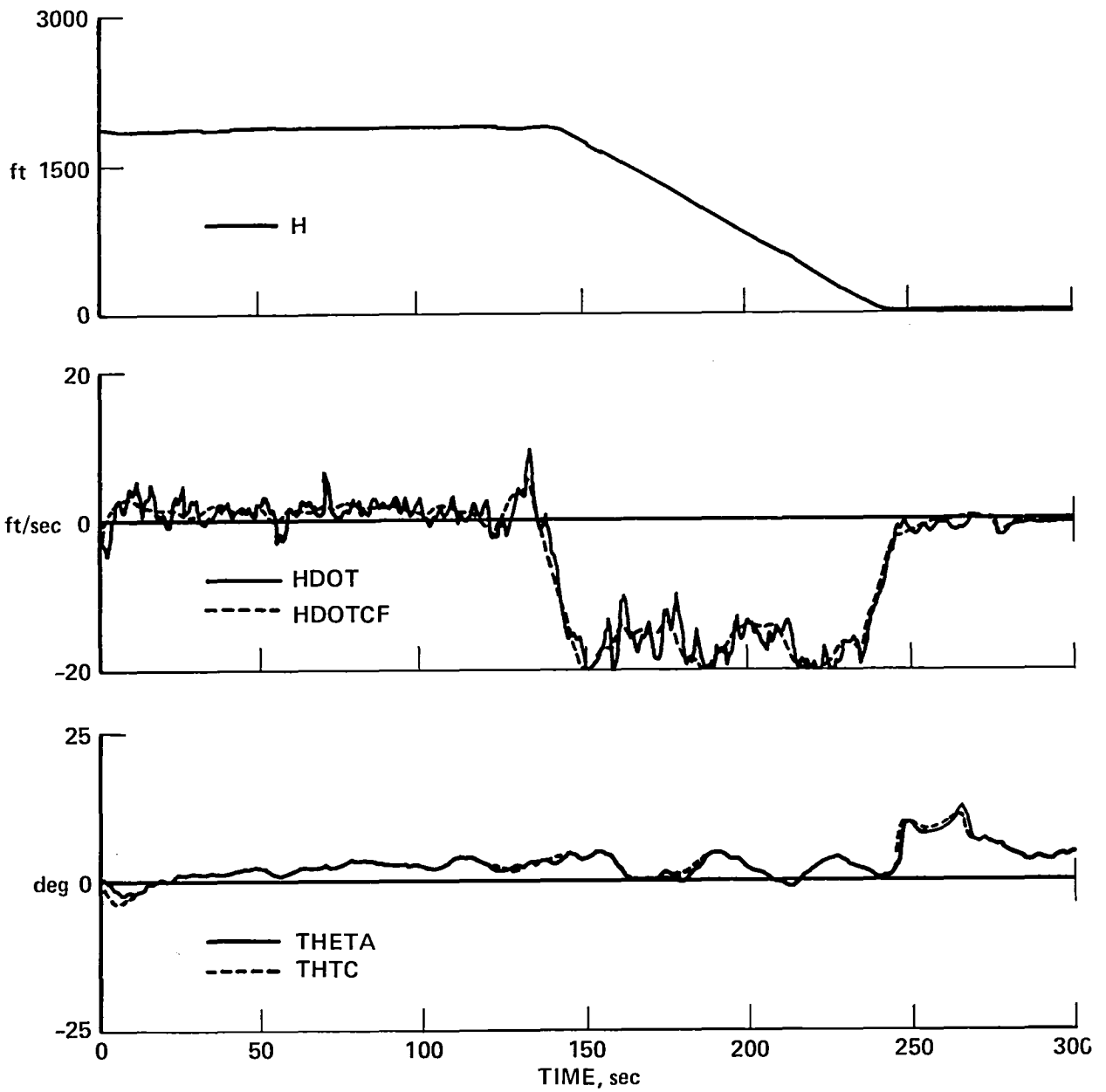

Figure 33.– Straight-in landing performance, 12.5° glide slope.

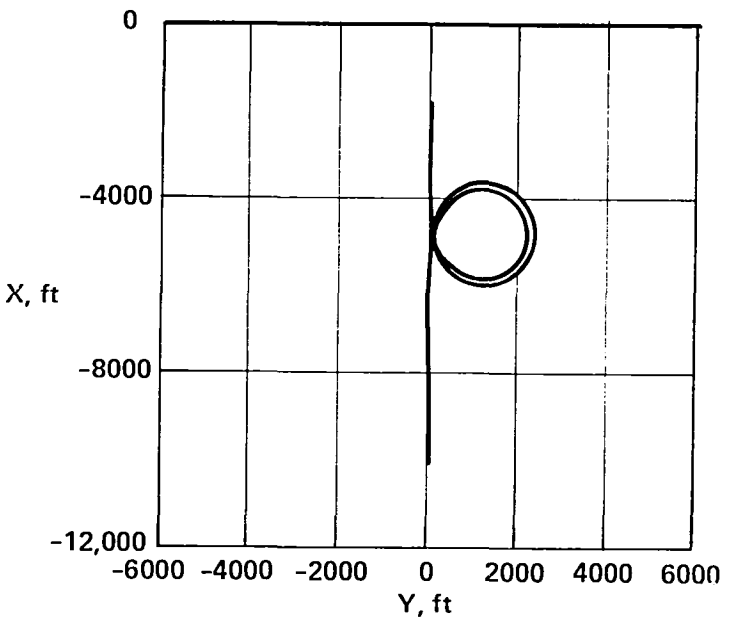

Figure 34.– X–Y plot of helix landing.

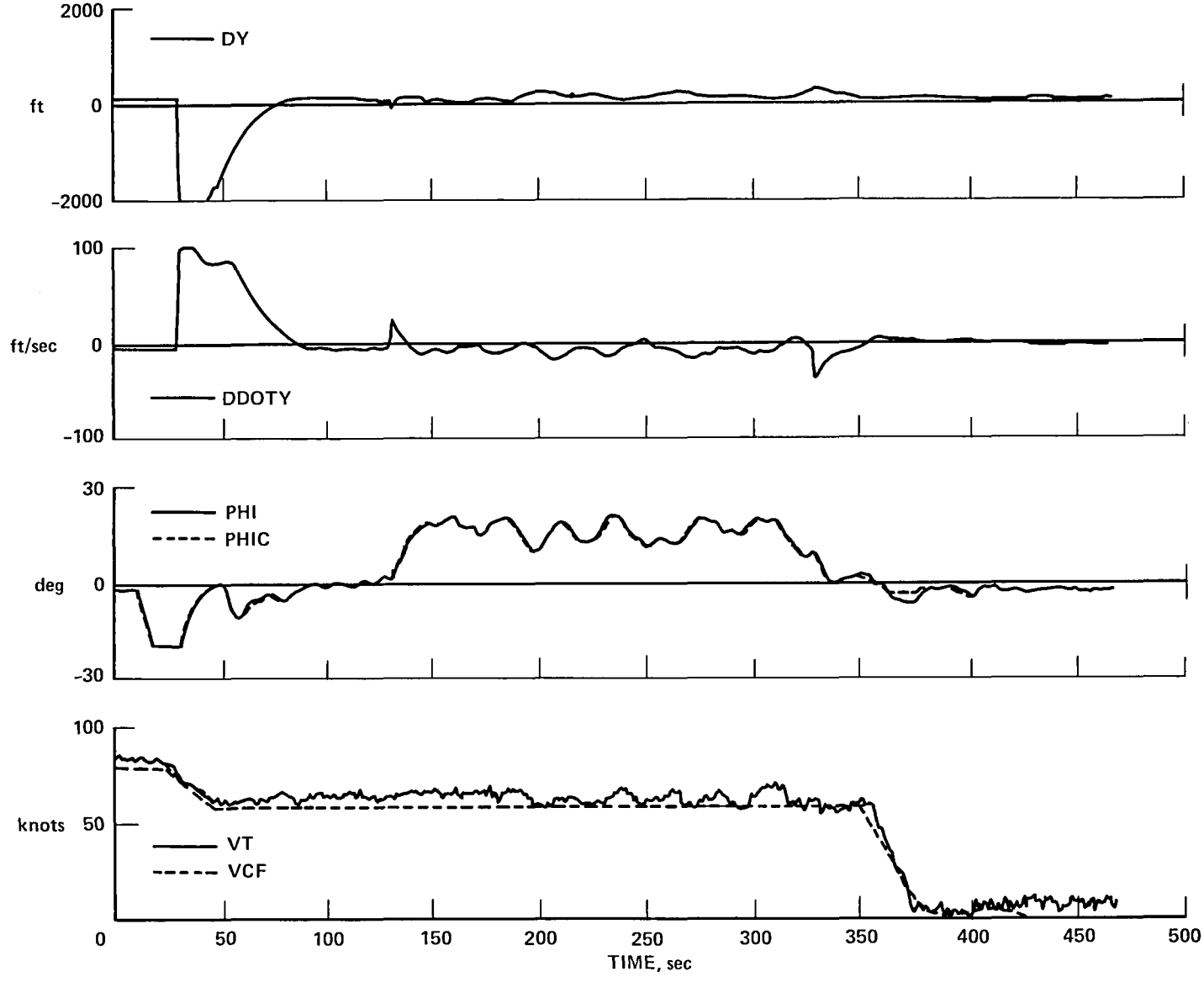

Figure 35.– Helix landing performance.

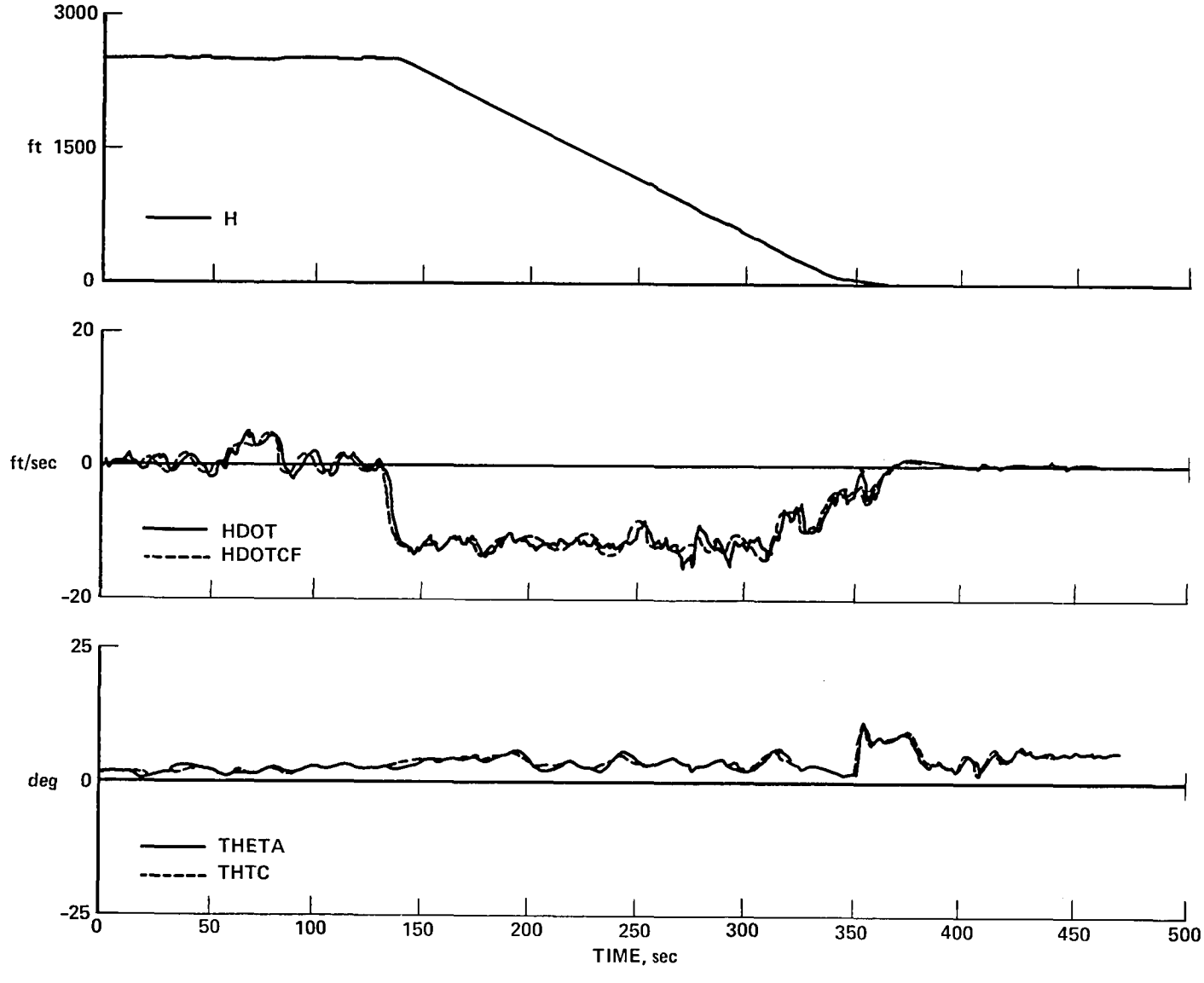

Figure 36.– Helix landing performance.

1. Report No. NASA TM-78591 AVRADCOM Tech. Rep. 79-23	2. Government Accession No.	3. Recipient's Catalog No.
4. Title and Subtitle V/STOLAND AVIONICS SYSTEM FLIGHT-TEST DATA ON A UH-1H HELICOPTER		5. Report Date February 1980 6. Performing Organization Code
7. Author(s) Fredric A. Baker,* Dean N. Jaynes,* Lloyd D. Corliss,† Sam Liden,‡ Robert B. Merrick,* and Daniel C. Dugan*		8. Performing Organization Report No. A-7831 10. Work Unit No. 513-54-11
9. Performing Organization Name and Address *Ames Research Center, NASA, Moffett Field, CA 94035 †AVRADCOM Research and Technology Laboratories, Moffett Field, CA 94035, and ‡Sperry Flight Systems Division, Sperry Rand Corporation, Phoenix, AZ 85002		11. Contract or Grant No. 13. Type of Report and Period Covered Technical Memorandum
12. Sponsoring Agency Name and Address National Aeronautics and Space Administration, Washington, D.C. 20546 and U.S. Army Aviation Research and Development Command, St. Louis, MO 93166		14. Sponsoring Agency Code

15. Supplementary Notes

16. Abstract

This report documents the flight-acceptance test results obtained during the acceptance tests of the V/STOLAND digital avionics system on a Bell UH-1H helicopter in 1977 at Ames Research Center. V/STOLAND is the acronym used for a versatile simplex digital avionics system developed and manufactured by Sperry Flight Systems Division of Sperry Rand Corporation. The system provides navigation, guidance, control, and display functions for NASA terminal area VTOL research programs and for the Army handling qualities research programs at Ames Research Center. The acceptance test verified system performance and contractual acceptability. The V/STOLAND hardware navigation, guidance, and control laws resident in the digital computers are described. Typical flight-test data are shown and discussed as documentation of the system performance at acceptance from the contractor.

17. Key Words (Suggested by Author(s))		18. Distribution Statement
Helicopter	Flight director	Unlimited
Flight-control system	Augmentation system	
Avionics	Navigation	
Digital	Guidance	
Fly-by-wire	Display	STAR Category – 08

19. Security Classif. (of this report)	20. Security Classif. (of this page)	21. No. of Pages	22. Price*
Unclassified	Unclassified	67	$5.25

*For sale by the National Technical Information Service, Springfield, Virginia 22161

NASA-Langley, 1980